© 2020. Published by The Company of Biologists Ltd | Journal of Cell Science (2020) 133, jcs242859. doi:10.1242/jcs.242859

RESEARCH ARTICLE

A cellular model of albumin endocytosis uncovers a link between membrane and nuclear proteins

Seiya Urae[1,2], Yutaka Harita[1,*], Tomohiro Udagawa[3], Koji L. Ode[4], Masami Nagahama[5], Yuko Kajiho[1], Shoichiro Kanda[1], Akihiko Saito[6], Hiroki R. Ueda[4,7], Masaomi Nangaku[2] and Akira Oka[1]

ABSTRACT

Cubilin (CUBN) and amnionless (AMN), expressed in kidney and intestine, form a multiligand receptor complex called CUBAM that plays a crucial role in albumin absorption. To date, the mechanism of albumin endocytosis mediated by CUBAM remains to be elucidated. Here, we describe a quantitative assay to evaluate albumin uptake by CUBAM using cells expressing full-length CUBN and elucidate the crucial roles of the C-terminal part of CUBN and the endocytosis signal motifs of AMN in albumin endocytosis. We also demonstrate that nuclear valosin-containing protein-like 2 (NVL2), an interacting protein of AMN, is involved in this process. Although NVL2 was mainly localized in the nucleolus in cells without AMN expression, it was translocated to the extranuclear compartment when coexpressed with AMN. NVL2 knockdown significantly impaired internalization of the CUBN-albumin complex in cultured cells, demonstrating an involvement of NVL2 in endocytic regulation. These findings uncover a link between membrane and nucleolar proteins that is involved in endocytic processes.

KEY WORDS: Cubilin, Amnionless, Nuclear valosin-containing protein-like, Albumin, Endocytosis

INTRODUCTION

Albumin, the most abundant circulating plasma protein, binds a wide variety of exogenous and endogenous molecules and has multiple physiological functions, including maintenance of colloid osmotic pressure, antioxidant activity and immune modulation (Quinlan et al., 2005; Spinella et al., 2016). Albumin is mainly synthesized in liver and its level is balanced by renal or gastrointestinal excretion and catabolism (Fanali et al., 2012; Naldi et al., 2017). Disruption of albumin homeostasis is associated with a variety of human diseases. In healthy kidneys, small amounts of serum albumin cross the glomerular filtration barrier and are efficiently reabsorbed by renal tubular cells under physiological conditions (Birn and Christensen, 2006; Gekle, 2005). Albuminuria occurs when the permeability of the glomerular capillary wall is increased or when reabsorption of albumin by tubular cells is impeded (Comper et al., 2008; Pollock and Poronnik, 2007). Clinically, the presence of albuminuria contributes to the progression of chronic kidney disease, and moderate albuminuria over time is also an important risk factor for cardiovascular disease and early cardiovascular mortality (Lambers Heerspink and Gansevoort, 2015; Parving et al., 2015).

Cubilin (CUBN), encoded by the *CUBN* gene, is one of the essential albumin receptors. CUBN is a 460 kDa multiligand receptor expressed in renal and intestinal epithelial cells (Amsellem et al., 2010; Birn et al., 2000; Christensen et al., 2013). Other ligands of CUBN include transferrin, intrinsic factor (IF)-vitamin B_{12}, hemoglobin, immunoglobulin light chain, apolipoprotein A-I and high-density lipoprotein (Batuman et al., 1998; Birn et al., 2000, 1997; Gburek et al., 2002; Gianesello et al., 2017; Hammad et al., 2000; Kozyraki et al., 1999; Kozyraki et al., 2001; Nagai et al., 2011; Nielsen et al., 2016). CUBN contains an N-terminal stretch, eight epidermal growth factor (EGF)-like repeats and 27 CUB [complement C1r/C1 s, Uegf (epidermal growth factor-related sea urchin protein) and BMP1 (bone morphogenic protein 1)] domains (Kozyraki et al., 1998; Moestrup et al., 1998). CUBN lacks a transmembrane domain and an intracellular domain (Moestrup et al., 1998) and thus requires another molecule, amnionless (AMN), to function as a receptor complex, called CUBAM (Fyfe et al., 2004; Kalantry et al., 2001; Tanner et al., 2003). AMN is a 38-50 kDa type I transmembrane protein that is expressed in intestine and kidney, where CUBN is also abundantly expressed (Strope et al., 2004). AMN has a cysteine-rich stretch in its extracellular domain and two [FY]XNPX[FY] endocytosis signal motifs in its intracellular domain (Fyfe et al., 2004; Kalantry et al., 2001), to which two adaptor proteins, autosomal recessive hypercholesterolemia protein (ARH, also known as LDLRAP1) and disabled-2 (DAB2), bind (Pedersen et al., 2010). In the absence of AMN, CUBN is retained in the endoplasmic reticulum (ER) and is unable to be targeted to the plasma membrane (Ahuja et al., 2008; Coudroy et al., 2005; Fyfe et al., 2004; He et al., 2005; Strope et al., 2004).

The crucial role of CUBN in ligand endocytosis in renal and intestinal tissues has been established in animal models and human disease. Cubilin-deficient mice exhibited markedly decreased uptake of albumin by proximal tubule cells and resultant albuminuria (Amsellem et al., 2010). In humans, several variants in *CUBN* are associated with albuminuria, suggesting the crucial function of CUBN in renal clearance of albumin (Boger et al., 2011; Teumer et al., 2016). Furthermore, loss-of-function mutations either in *CUBN* or *AMN* are reported to cause the congenital disease Imerslund–Grasbeck syndrome (IGS), also known as juvenile megaloblastic anemia 1 (MGA1) (OMIM #261100) (Aminoff et al.,

[1]Department of Pediatrics, Graduate School of Medicine, The University of Tokyo, Bunkyo-ku, Tokyo 113-8655, Japan. [2]Division of Nephrology and Endocrinology, The University of Tokyo, Bunkyo-ku, Tokyo 113-8655, Japan. [3]Department of Pediatrics and Developmental Biology, Graduate School of Medical and Dental Sciences, Tokyo Medical and Dental University, Bunkyo-ku, Tokyo 113-8510, Japan. [4]Department of Systems Pharmacology, Graduate School of Medicine, The University of Tokyo, Bunkyo-ku, Tokyo 113-8654, Japan. [5]Laboratory of Molecular and Cellular Biochemistry, Meiji Pharmaceutical University, Kiyose-shi, Tokyo 204-8588, Japan. [6]Department of Applied Molecular Medicine, Niigata University Graduate School of Medical and Dental Sciences, Niigata-shi, Niigata 951-8510, Japan. [7]Laboratory for Synthetic Biology, RIKEN Center for Biosystems Dynamics Research, Wako-shi, Saitama 351-0198, Japan.

*Author for correspondence (haritay-ped@h.u-tokyo.ac.jp)

Y.H., 0000-0002-3123-7444; T.U., 0000-0002-7177-6426

Handling Editor: Jennifer Lippincott-Schwartz
Received 13 December 2019; Accepted 20 May 2020

Journal of Cell Science (2020) 133, jcs242859. doi:10.1242/jcs.242859

1999; Tanner et al., 2003, 2012). Patients with IGS present with low molecular weight proteinuria and megaloblastic anemia as a result of impaired IF-vitamin B_{12} complex absorption in ileum (Gräsbeck, 2006; Tanner et al., 2012). One pathogenic mechanism of IGS is the disruption of correct intracellular trafficking of CUBAM to the cell membrane (Amsellem et al., 2010; Coudroy et al., 2005; Fyfe et al., 2004, 1991; He et al., 2005; Storm et al., 2011; Strope et al., 2004). We previously reported that AMN-dependent glycosylation of CUBN is crucial for membrane targeting (Udagawa et al., 2018) and several mutations of *CUBN* and *AMN* result in abrogation of AMN-dependent plasma membrane localization of CUBN (Udagawa et al., 2018). Another mechanism of IGS is inhibition of ligand binding to CUBN by mutations within its vitamin B_{12}/IF-binding region (CUB5-8) (Andersen et al., 2010; Tanner et al., 2012).

So far, the mechanism underlying the endocytosis of albumin by CUBN has remained controversial. Previous biochemical studies have identified two distinct domains in CUBN that directly bind to albumin: the 113 amino acid (aa) N-terminal stretch and the CUB 7 and CUB 8 domains (Yammani et al., 2001). However, accumulating evidence in humans suggests that mutations or variants in the C-terminal part (CUB9-27 domains) of CUBN rather than the CUB5-8 domains are associated with albuminuria (Ahluwalia et al., 2019; Bedin et al., 2020; Boger et al., 2011; Haas et al., 2018; Teumer et al., 2016; Zanetti et al., 2019). To date, the role the C-terminal CUB domains of CUBN in albumin endocytosis has not been experimentally demonstrated.

Albumin endocytosis in renal tubular cells is also regulated by another CUBN-binding protein, megalin (also known as LRP-2), a large transmembrane protein that belongs to the LDL receptor family (Eshbach and Weisz, 2017). Megalin forms a trimetric complex with CUBN and AMN (Ahuja et al., 2008) and also bears endocytosis signal motifs on its intracellular domain (Saito et al., 1994). By using genetic mouse models, megalin was shown to promote endocytosis of the CUBN-albumin complex (Amsellem et al., 2010). Although AMN is essential for surface expression of CUBN, whether AMN is involved in CUBN-mediated albumin endocytosis is not clear. Furthermore, the regulatory mechanism of CUBN-mediated endocytosis is poorly understood.

In the present study, we establish a quantitative assay to evaluate cellular albumin uptake in cultured cells mediated by CUBAM. We demonstrate that the C-terminal part of CUBN and the signal motifs of AMN are crucial for albumin endocytosis. We also identify nuclear valosin-containing protein-like 2 (NVL2) as a novel interacting protein of AMN and show that NVL2 is involved in CUBN-mediated endocytosis of albumin. Our findings reveal a novel function of a nucleolar protein in regulating ligand endocytosis through a cell surface receptor.

RESULTS

Full-length CUBN facilitates albumin endocytosis

To analyze intracellular traffic or endocytosis by CUBAM in cultured cells, several short forms of CUBN have been used, including N-terminal CUBN fragments composed of the 113 aa N-terminal stretch, EGF repeats and the CUB1-4 domain [mini-CUBN (1-4)] (Udagawa et al., 2018) (Fig. 1A) or CUB1-8 domain [mini-CUBN (1-8)] (Coudroy et al., 2005; Fyfe et al., 2004) (Fig. S1A). We generated a mammalian expression vector encoding full-length human CUBN with a FLAG-tag on its C terminus (Fig. 1A). The full-length CUBN expressed in HEK293 T cells interacted with AMN (Fig. 1B) and was targeted to the cell membrane only when AMN was coexpressed (Fig. 1C), similar to mini-CUBNs (Udagawa et al., 2018).

The albumin endocytosis capacity of full-length CUBN was compared with that of mini-CUBN (1-4) or mini-CUBN (1-8). Cells expressing mini-CUBN (1-4), mini-CUBN (1-8) or full-length CUBN (Fig. S1A,B) were incubated in medium containing FITC-bovine serum albumin (BSA) for 1 h. The amounts of albumin endocytosed in the cells and CUBN expressed on cell surface were quantified by immunostaining without permeabilization. Cells expressing full-length CUBN, but not those expressing mini-CUBN (1-4) at the cell surface, demonstrated significantly increased internalization of albumin compared with CUBN-negative cells (Fig. 1D). Internalization of albumin by full-length CUBN was also confirmed by flow cytometry analysis (Fig. 1E,F). Although a previous study demonstrated that the CUB 7-8 domain of CUBN binds to albumin (Yammani et al., 2001), expression of mini-CUBN (1-8) failed to increase the cellular uptake of albumin (Fig. S1C,D). In cells expressing full-length CUBN, the signals of internalized albumin were colocalized with internalized CUBN and partially colocalized with EEA1, an early endosome marker (Mu et al., 1995) (Fig. 1G). These results suggest that albumin is internalized by full-length CUBN, but not by the N-terminal mini-CUBN (1-8), and colocalizes with CUBN in early endosomes.

Signal motifs of AMN are crucial for albumin endocytosis by CUBN

AMN has two signal motifs in its intracellular domain that are essential for internalization of the IF-vitamin B_{12} complex mediated by CUBAM (Pedersen et al., 2010). The AMN mutant that lacks both signal motifs (Sdel-AMN) (Fig. 2A) bound to CUBN and promoted CUBN membrane targeting in the same manner as wild-type AMN (Fig. 2B; Fig. S2A,B). However, cells expressing Sdel-AMN together with full-length CUBN demonstrated significantly impaired albumin uptake (Fig. 2C,D), suggesting that the endocytosis signal motifs of AMN are crucial for CUBAM-mediated albumin uptake.

To investigate whether the internalization of CUBAM is dependent on megalin, the endocytosis assay was performed in human cultured colorectal HCT116 cells, which do not express endogenous *megalin* mRNA (Udagawa et al., 2018). CUBN endocytosis dependency on AMN signal motifs was also observed in HCT116 cells, suggesting that CUBAM endocytosis occurs independently of megalin expression (Fig. S2C,D).

NVL2 is a novel interacting partner of AMN

To investigate the regulatory mechanism of albumin endocytosis mediated by CUBAM, an interactome analysis of AMN using stable isotope labeling by amino acids in cell culture (SILAC) technology was performed (Fig. 3A). AMN was expressed in HEK293T cells that were cultured in medium containing heavy isotope-labeled amino acids, and empty vector was transfected into cells cultured in medium containing light isotope-labeled amino acids. The lysates from both cell samples were mixed, immunoprecipitated and subjected to nanoscale liquid chromatography coupled with tandem mass spectrometry (nano-LC-MS/MS). Nuclear valosin-containing protein-like (NVL) was among the candidate molecules interacting with AMN that contained higher ratios of heavy/light amino acids (Fig. 3B,C).

NVL is an AAA-ATPase (ATPase associated with various cellular activities). The human genome encodes two isoforms, NVL1 and NVL2, which are identical over the 750 C-terminal amino acids (Fig. 3D) (Germain-Lee et al., 1997). Although the physiological role of NVL1 has not been clarified, NVL2 has been reported to localize in the cell nucleolus and function in ribosome

Journal of Cell Science (2020) 133, jcs242859. doi:10.1242/jcs.242859

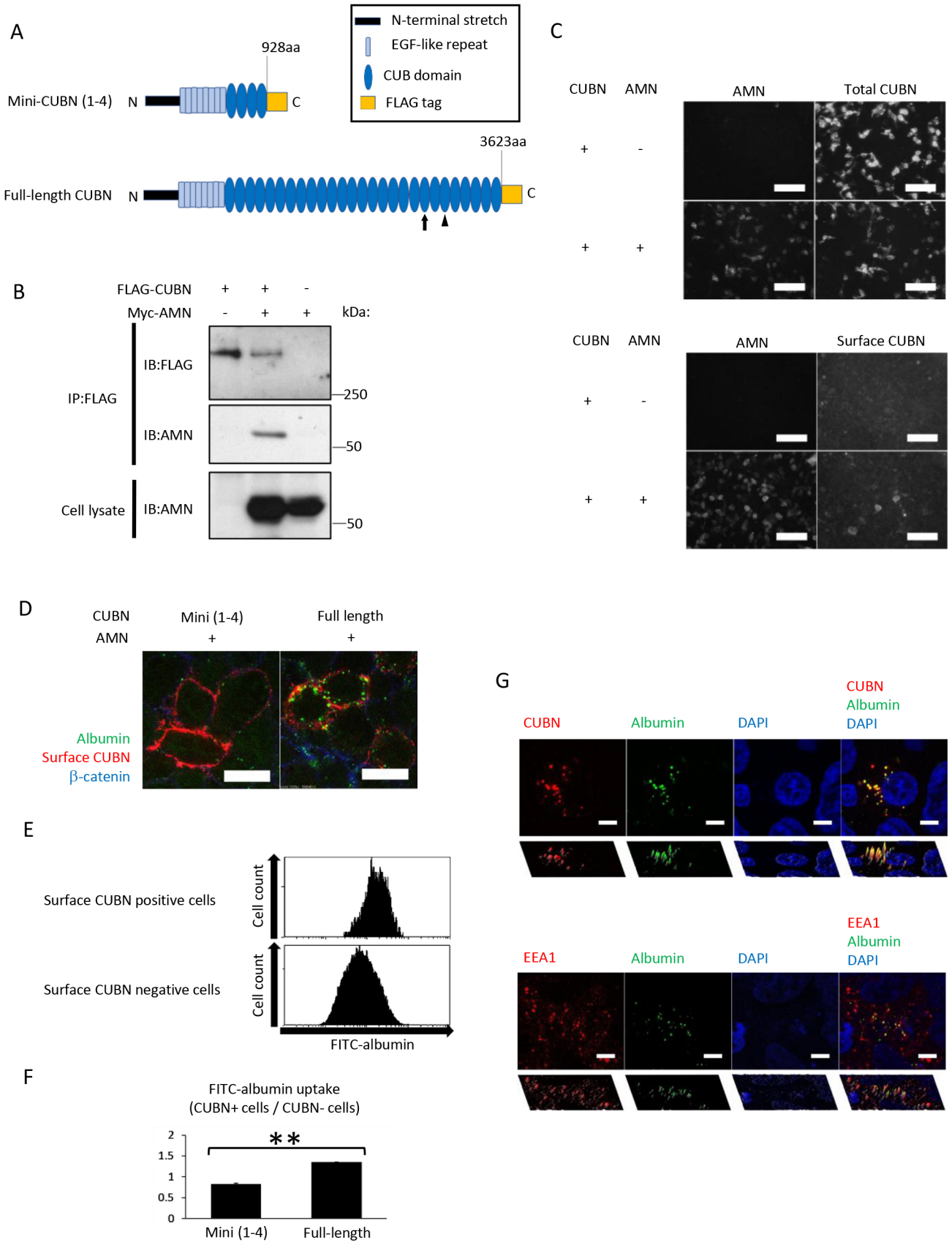

Fig. 1. See next page for legend.

Journal of Cell Science (2020) 133, jcs242859. doi:10.1242/jcs.242859

Fig. 1. Full-length CUBN facilitates albumin uptake by cultured cells. (A) Representation of mini-CUBN (1-4) and full-length CUBN. The arrow and arrowhead indicate the locations of a mutation (p.S2785fsX19) found in a patient with proteinuria (Ovunc et al., 2011) and a polymorphism (p.I2984V) associated with albuminuria (Boger et al., 2011; Tanner et al., 2012; Teumer et al., 2016), respectively. (B) Co-immunoprecipitation of FLAG-tagged full-length CUBN and myc-tagged AMN exogenously expressed in HEK293T cells. (C) Total expression (upper panels) and surface expression (lower panels) of FLAG-tagged full-length CUBN in HEK293T cells with or without myc-GFP-tagged AMN co-expression. (D) FITC-albumin uptake by HEK293T cells expressing FLAG-tagged mini-CUBN (1-4) or full-length CUBN with myc-tagged AMN. Cells were immunostained for β-catenin and surface FLAG-tagged CUBN after FITC-albumin uptake. (E) FITC-albumin uptake by HEK293T cells expressing CUBN on the surface was analyzed by flow cytometry. Cells were divided into CUBN-positive and CUBN-negative groups according to fluorescent intensity. (F) Flow cytometric quantification of FITC-albumin uptake by HEK293T cells. Median intensities of FITC in mini-CUBN (1-4)- or full-length CUBN-positive cells normalized to that of CUBN-negative cells were calculated. Data are shown as mean±s.e.m. (n=3). **P<0.01, using a two-sided t-test. (G) Colocalization of internalized FITC-albumin with FLAG-tagged CUBN and endogenous EEA1, a marker for early endosomes. Scale bars: 100 µm (C), 10 µm (D), 5 µm (G).

synthesis and telomerase activity (Her and Chung, 2012; Nagahama et al., 2004). Immunoprecipitation assays revealed that NVL2 but not NVL1 interacts with AMN (Fig. 3E; Fig. S3A,B). An interaction between endogenous NVL2 and AMN was also confirmed in CACO2 cells (Fig. 3F).

AMN regulates the intracellular localization of NVL2

In HEK293T cells, which do not express endogenous AMN (Fig. S4A), endogenous NVL is located in the nuclear compartment. However, when AMN is overexpressed in these cells, endogenous NVL translocates to the extranuclear compartment (Fig. 4A). Proximity ligation assay (PLA), which detects the approximation of two molecules within 40 nm, showed signals indicating the proximity of AMN and NVL2 in the extranuclear compartment (Fig. 4B). Co-immunostaining with calnexin (CNX), an ER marker (Wada et al., 1991), revealed that NVL colocalized with AMN in the ER in AMN-expressing cells (Fig. 4C). CUBN and AMN are interdependently targeted to the plasma membrane (Fyfe et al., 2004; Udagawa et al., 2018). We also analyzed the localization of NVL2 and its interaction with AMN in cells expressing both CUBN and AMN. In cells coexpressing NVL2, AMN and CUBN, NVL2 partially colocalizes with β-catenin along the cell membrane (Ozawa et al., 1989) (Fig. 4D). PLA assay with co-staining of CNX or β-catenin showed the proximity of AMN and NVL2 both in the ER and along the plasma membrane in CUBAM-expressing cells (Fig. 4E,F). Furthermore, the interaction between NVL2 and CUBN along the cell surface was analyzed using cells expressing wild-type CUBN or the G653R mutant, which is defective in trafficking to the cell surface (Udagawa et al., 2018). HEK293T cells transiently expressing FLAG-tagged wild-type or mutant CUBN along with exogenous NVL2 and AMN were incubated in medium containing anti-FLAG antibody so that CUBN on the cell surface was labeled (Fig. S3C). Cell lysates were incubated with Protein G Sepharose beads, and bound proteins were analyzed by western blotting. In cells expressing the CUBN G653R mutant, levels of CUBN on the cell surface as well as AMN and NVL2 bound to CUBN on the cell surface were markedly reduced compared with cells expressing wild-type CUBN. These results demonstrate that NVL2 is expressed in extranuclear compartments, such as the ER and plasma membrane, in cells expressing AMN and CUBN.

In human renal tubules and intestine, NVL was located mainly in the nucleolus. However, distinct signals for NVL were also detected in the extranuclear compartment, colocalizing with AMN signals (Fig. 4G-I; Fig. S5).

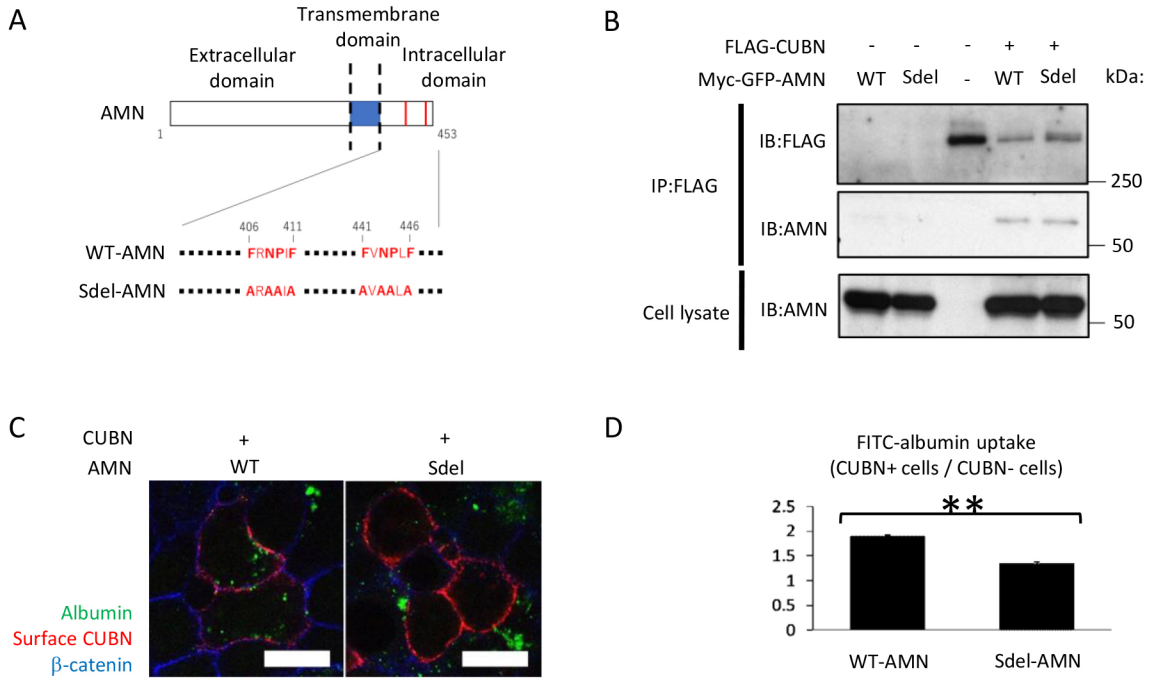

Fig. 2. Signal motifs of AMN are critical for albumin uptake by CUBN. (A) Representation of the endocytosis signal motifs in the intracellular domain of AMN. Signal motifs were mutated in Sdel-AMN. (B) Co-immunoprecipitation of FLAG-tagged full-length CUBN with myc-GFP-tagged wild-type (WT)-AMN or Sdel-AMN exogenously expressed in HEK293T cells. (C) FITC-albumin uptake by HEK293T cells expressing FLAG-tagged full-length CUBN with WT-AMN or Sdel-AMN. (D) Flow cytometric quantification of FITC-albumin uptake by HEK293T cells expressing full-length CUBN with WT-AMN or Sdel-AMN. Data are shown as mean±s.e.m. (n=3). **P<0.01, using a two-sided t-test. Scale bars: 10 µm.

Journal of Cell Science (2020) 133, jcs242859. doi:10.1242/jcs.242859

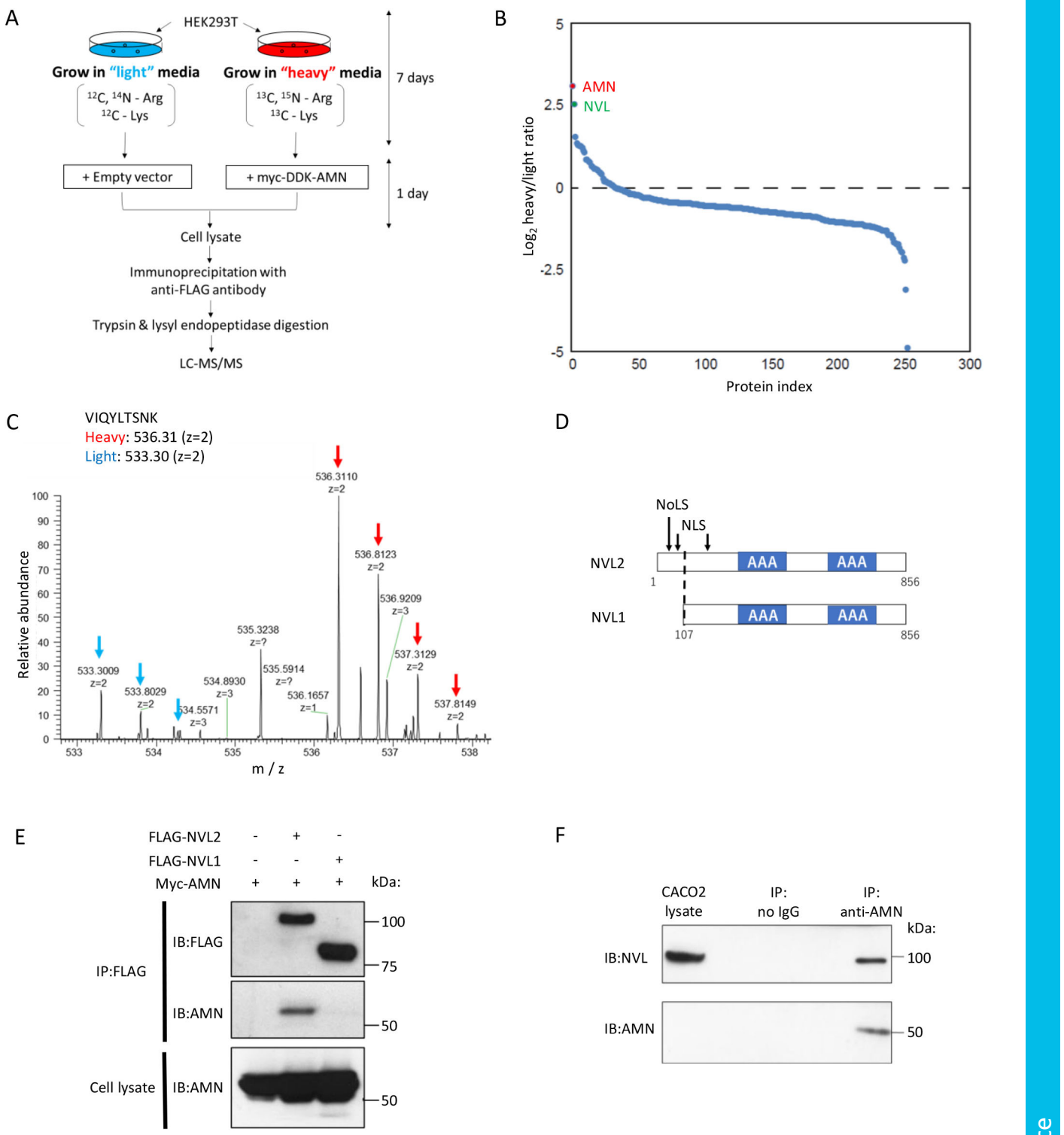

Fig. 3. NVL2 is a novel interacting partner of AMN. (A) Scheme for SILAC labeling and proteome analysis for the identification of AMN-interacting proteins. (B) SILAC heavy/light ratios of identified proteins. The quantified SILAC ratios of proteins identified with more than five peptide-spectrum matches (PSM) are shown. (C) Representative spectral data of a peptide derived from NVL (VIQYLTSNK). (D) Representation of NVL1 and NVL2. (E) Co-immunoprecipitation of myc-tagged AMN with FLAG-tagged NVL1 or NVL2 exogenously expressed in HEK293T cells. (F) Co-immunoprecipitation of endogenous AMN and NVL2 in CACO2 cells.

Signal motifs of AMN and the N-terminal domain of NVL2 are necessary for their interaction

To explore further the physical association of NVL2 and AMN, we analyzed the domain of AMN responsible for its interaction with NVL2 (Fig. 5A). Immunoprecipitation assay demonstrated that elimination of the intracellular domain of AMN (AMN-ΔICD) remarkably impaired its interaction with NVL2 (Fig. 5B). Pull-down analysis demonstrated that the intracellular domain of AMN (AMN-ICD) was sufficient to interact with NVL2 (Fig. 5C). Elimination of signal motifs in AMN-ICD (Fig. 2A) completely

Journal of Cell Science (2020) 133, jcs242859. doi:10.1242/jcs.242859

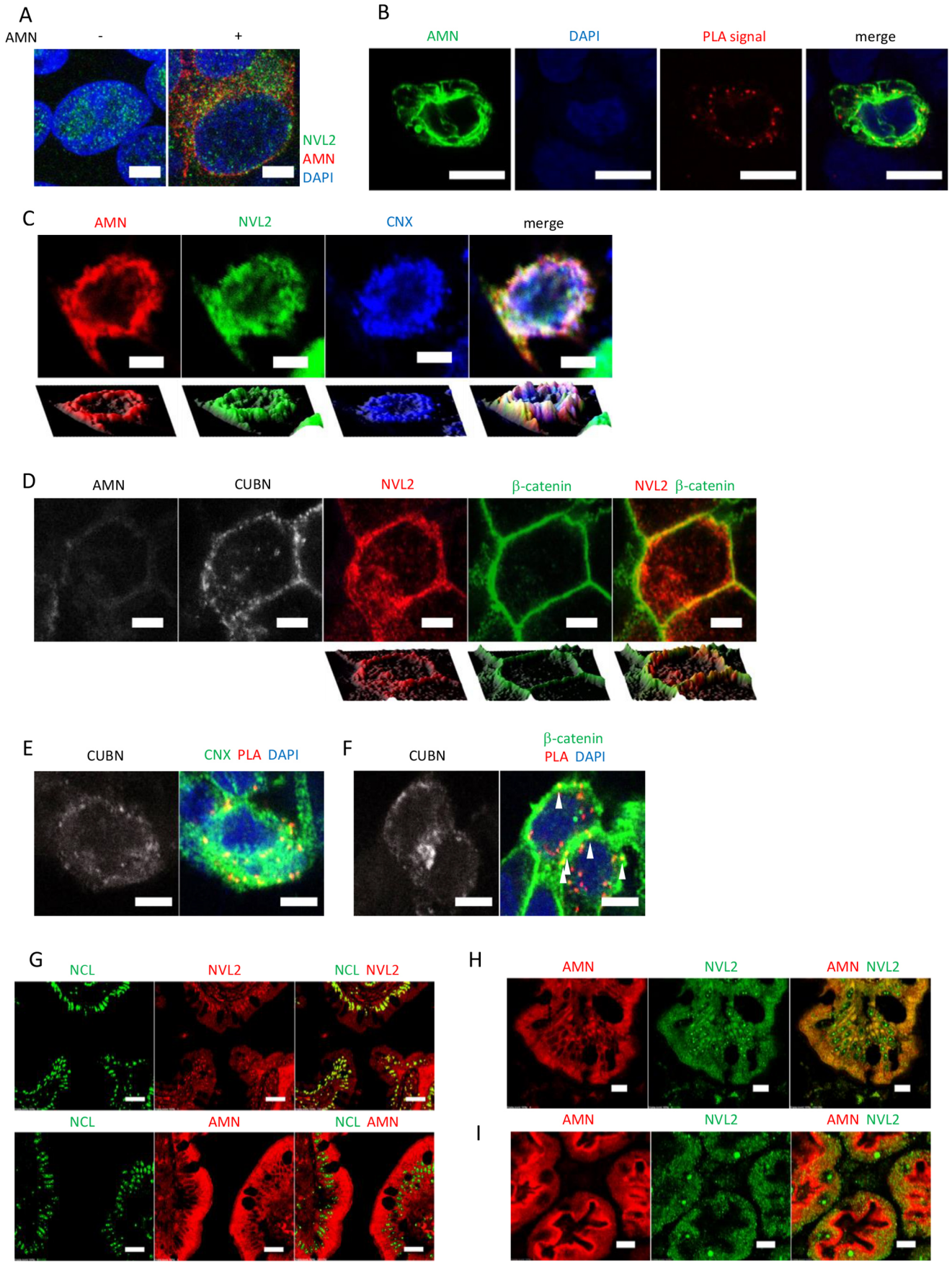

Fig. 4. See next page for legend.

Journal of Cell Science (2020) 133, jcs242859. doi:10.1242/jcs.242859

Fig. 4. AMN regulates intracellular localization of NVL. (A) Location of endogenous NVL in HEK293T cells with or without myc-DDK-tagged AMN overexpression. (B) *In situ* proximity ligation assay (PLA) in HEK293T cells expressing myc-GFP-tagged AMN and FLAG-tagged NVL2. (C) Colocalization of exogenously expressed myc-DDK-AMN, endogenous NVL and the ER marker calnexin (CNX) in HEK293T cells. (D) Colocalization of exogenously expressed HA-tagged NVL2 and β-catenin along the plasma membrane in HEK293T cells co-expressing myc-tagged AMN and FLAG-tagged mini-CUBN (1-4). (E,F) *In situ* PLA of myc-GFP-tagged AMN and FLAG-tagged NVL2 in HEK293T cells co-expressing GFP-tagged CUBN. Cells were co-immunostained for endogenous CNX (E) or β-catenin (F) after the PLAs. Arrowheads in F indicate proximity signals colocalized with β-catenin along the plasma membrane. (G) Localization of NVL (top) and AMN (bottom) in intestine epithelia co-stained for nucleolin (NCL), a nucleolar marker. (H,I) Colocalization of AMN and NVL in the cytoplasm of intestine epithelial cells (H) or renal tubular cells (I). Scale bars: 5 µm (A,C,D), 10 µm (B,E,F,H,I), 20 µm (G).

abrogated its interaction with NVL2 (Fig. 5D), and Sdel-AMN did not cause the translocation of NVL into cytoplasm that was observed with wild-type AMN (Fig. 5E). Therefore, both interaction of AMN and NVL2 and cytoplasmic translocation of NVL are dependent on the intracellular endocytosis signal motifs of AMN.

Because the signal motifs of AMN mediate endocytosis of CUBAM through interactions with the adaptor molecules ARH and Dab2 (Pedersen et al., 2010), we examined the interaction between NVL2 and the adaptor proteins by immunoprecipitation. Although we could not detect an interaction between NVL2 and Dab2, NVL2 bound to ARH only when AMN was coexpressed (Fig. S6A). PLA assay also confirmed the proximity of NVL2 and ARH in cells expressing AMN (Fig. S6C). The signals indicating the AMN-dependent proximity of NVL2 and ARH in CUBAM-expressing cells were partly colocalized with β-catenin along the plasma membrane (Fig. S6D). These results suggest that the intracellular signal motifs of AMN mediate formation of the NVL2-AMN-ARH trimeric complex along the plasma membrane.

We also investigated the domains of NVL2 that are responsible for its interaction with AMN (Fig. 5F). Immunoprecipitation assays demonstrated that elimination of the N terminus of NVL2 (NVL2-D1D2) remarkably impaired its interaction with AMN (Fig. 5G), suggesting that the N terminus of NVL2 is the domain essential for its interaction with AMN. Pull-down analysis demonstrated that the recombinant N terminus of NVL2 (NVL2-NT) was sufficient to interact with AMN (Fig. 5H).

NVL2 is an AAA-ATPase with two functional ATPase domains (AAA domains) in the central region (D1) and the C terminus (D2). We investigated whether the capacity of NVL2 for ATP hydrolysis or ATP binding influences the interaction between NVL2 and AMN. We used NVL2 with E365Q or E682Q mutation, which impairs the ATP-hydrolysis capacity of the AAA domain in D1 or D2, respectively, and NVL2 with K311M or K628M mutation, which impairs the ATP-binding capacity of the AAA domain in D1 or D2, respectively (Fig. 5F) (Lo et al., 2019). Immunoprecipitation assays showed that although the NVL2 mutants deficient in ATP hydrolysis (E365Q, E682Q or E365Q/E682Q) still interacted with AMN, the K311M or K311M/K628M mutation in NVL2 clearly disturbed its interaction with AMN (Fig. 5I). NVL2-AMN-ARH trimeric complex formation was also impaired by K311M mutation (Fig. S6B). These data indicated that although the N terminus plays an essential role in the interaction between NVL2 and AMN, the ATP-binding state of NVL2 influences the interaction with AMN.

NVL2 facilitates endocytosis of CUBN

To investigate the involvement of NVL2 in the endocytosis of CUBAM, we depleted NVL in HEK293T cells transiently expressing CUBN and AMN (Fig. 6A). Knockdown of endogenous NVL did not inhibit membrane targeting of CUBN (Fig. 6B).

We then examined the role of NVL on the endocytosis of CUBAM by endocytosis assay (Pedersen et al., 2010). FLAG-tagged mini-CUBN (1-4) on the cell surface was labeled with anti-FLAG antibody and incubated for 1 h at 37°C. Endocytosed CUBN molecules were detected by secondary antibody in the form of signals internalized into the cells. In control cells transfected with control siRNA, almost all the signals for CUBN were internalized after 1 h (Fig. 6C). On the other hand, internalized CUBN in two lines of NVL knockdown cells was decreased compared with control cells (Fig. 6C). We quantitatively evaluated the proportion of CUBN that was left on the cell surface after induction of endocytosis by calculating the proportion of CUBN that colocalized with β-catenin along the cell membrane (Ozawa et al., 1989). The proportion of CUBN left on the cell surface was significantly increased in NVL-depleted cells compared with control cells (Fig. 6D,E). The reduced CUBN internalization caused by NVL depletion was rescued by expression of siRNA-resistant NVL2 (Fig. 6F,G), confirming that NVL2 facilitates endocytosis of CUBN.

NVL2 facilitates CUBAM-mediated albumin endocytosis

We also evaluated the functional influence of NVL on albumin uptake mediated by CUBAM. HEK293T cells expressing full-length CUBN and AMN with or without NVL knockdown were incubated in medium containing FITC-labeled BSA at 37°C for 1 h. Surface CUBN and β-catenin were visualized by immunostaining. In cells transfected with control siRNA, most of the albumin was internalized into the cells. In contrast, significant amounts of albumin were retained on the surface of NVL-depleted cells (Fig. 7A). Flow cytometry analysis demonstrated that uptake of FITC-BSA was significantly decreased in NVL knockdown cells compared with control cells (Fig. 7B). We also quantified the proportion of FITC-BSA retained on the cell surface by calculating the signals for CUBN on the cell surface colocalized with β-catenin. Significantly higher proportions of FITC-BSA signals were retained on the cell surface in NVL-depleted cells compared with control cells (Fig. 7C). The surface retention of albumin in NVL-depleted cells was rescued by expression of siRNA-resistant NVL2 (Fig. 7D). The role of NVL in albumin uptake was also confirmed in CACO2 cells, which express endogenous CUBN and AMN (Fig. S4B, Fig. S7A,B).

Involvement of the ATPase activity of NVL2 on CUBAM-mediated albumin uptake was also evaluated using cells expressing doxycycline (Dox)-inducible NVL2 (wild-type or E365Q/E682Q) (Yoshikatsu et al., 2015). Albumin uptake by cells expressing E365Q/E682Q NVL2 was significantly impaired (Fig. 7E,F) compared with cells expressing wild-type NVL2, suggesting that the ATP-hydrolysis capacity of NVL2 plays a crucial role in its regulation of CUBAM-mediated albumin endocytosis.

Because NVL2 is reported to play a role in ribosome biosynthesis (Nagahama et al., 2004, 2006), we examined whether impaired albumin uptake by NVL depletion was mediated by nucleolar stress (Boulon et al., 2010). Administration of actinomycin D or CX-5461, both of which inhibit Pol I-driven rRNA transcription (Carmo-Fonseca et al., 1992; Drygin et al., 2011), induced the release of nucleolin in the nucleoplasm (Fig. S8A), which indicated nucleolar disruption (Boulon et al., 2010). Notably, actinomycin D or CX-5461 did not affect CUBAM-mediated albumin uptake (Fig. S8B). These results suggest that reduced CUBAM-mediated albumin uptake caused by NVL depletion is not mediated by nucleolar stress.

Journal of Cell Science (2020) 133, jcs242859. doi:10.1242/jcs.242859

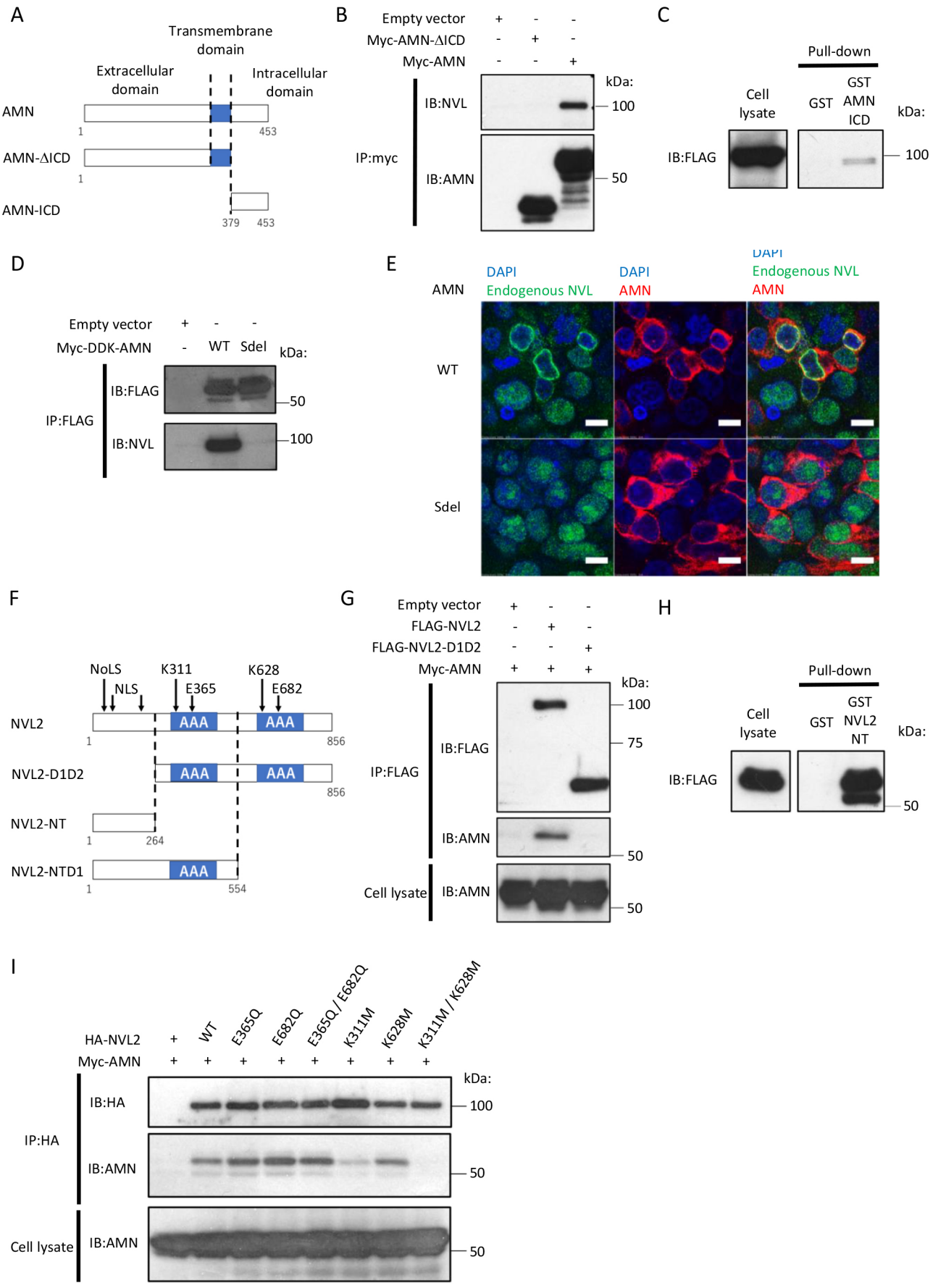

Fig. 5. See next page for legend.

Journal of Cell Science

Journal of Cell Science (2020) 133, jcs242859. doi:10.1242/jcs.242859

Fig. 5. Endocytosis signal motifs in the AMN intracellular domain and the N terminus of NVL2 are essential for their interaction. (A) Representation of full-length and short forms of AMN (AMN-ΔICD and AMN-ICD). (B) Co-immunoprecipitation of endogenous NVL2 with myc-tagged full-length AMN or AMN-ΔICD exogenously expressed in HEK293T cells. (C) Pull-down of NVL2 by recombinant GST-tagged AMN-ICD. GST-tagged AMN-ICD and GST were generated in *E. coli*, purified using glutathione Sepharose beads and incubated with lysates of HEK293T cells transfected with FLAG-NVL2. (D) Co-immunoprecipitation of endogenous NVL2 with myc-DDK-tagged wild-type (WT)-AMN or Sdel-AMN expressed in HEK293T cells. (E) Localization of endogenous NVL in HEK293T cells expressing myc-DDK-tagged WT-AMN (top) or Sdel-AMN (bottom). (F) Representation of full-length and truncated forms of NVL2 (NVL2-D1D2, NVL2-NT and NVL2-NTD1). (G) Co-immunoprecipitation of myc-tagged AMN with FLAG-tagged full-length NVL2 or NVL2-D1D2 exogenously expressed in HEK293T cells. (H) Pull-down of AMN by recombinant GST-tagged NVL2-NT. GST-tagged NVL2-NT and GST were generated in *E. coli*, purified using glutathione Sepharose beads and incubated with lysates of HEK293T cells transfected with myc-DDK-tagged AMN. (I) Co-immunoprecipitation of myc-tagged AMN with HA-tagged WT or mutant NVL2 exogenously expressed in HEK 293T cells. Scale bars: 10 µm.

DISCUSSION

Here, we have established a cellular model in which full-length CUBN is expressed on the cell surface to enable quantitative evaluation of albumin uptake. Our findings reveal a novel regulatory mechanism of endocytosis that is controlled by CUBN, AMN and NVL2 (Fig. 8).

Previous *in vitro* analyses using segmented fragments identified two distinct domains in CUBN that directly bind to albumin: the 113 aa N-terminal stretch and CUB 7 and CUB 8 domains (Yammani et al., 2001). However, the CUBN fragment comprising the N-terminal stretch, EGF repeats and CUB 1-8 domain was not sufficient for endocytosis of albumin in cultured cells (Fig. S1C,D). A previous study reported a patient with single-base homozygous deletion (c.8355delA) in exon 53 of CUBN, causing premature truncation of the encoded protein (p.S2785fsX19) in the CUB 20 domain; this patient presented proteinuria, but not anemia, suggesting that deletion of C-terminal CUB domains affects albumin uptake without interfering with IF-vitamin B_{12} endocytosis (Ovunc et al., 2011). Other biallelic variants in the C terminus of CUBN have also been found in patients with isolated proteinuria (Bedin et al., 2020). Furthermore, recent GWAS studies identified polymorphisms affecting the C-terminal CUB domains (p.A1690V, p.N2157D, p.I2984V, p.A2914V) that are associated with albuminuria (Ahluwalia et al., 2019; Boger et al., 2011; Haas et al., 2018; Teumer et al., 2016; Zanetti et al., 2019). Our results have experimentally demonstrated the crucial role of the C-terminal CUB domains of CUBN in albumin endocytosis and provide theoretical basis for these genotype–phenotype associations.

Regarding the role of AMN in endocytosis, the intracellular signal motifs of AMN have been shown to be essential for the uptake of IF-vitamin B_{12} complex, which binds to CUB 5-8 domains of CUBN (Pedersen et al., 2010). Because IF does not bind to megalin, AMN is thought to mediate internalization of the IF-vitamin B_{12} complex in a megalin-independent manner (Fyfe et al., 2004; Pedersen et al., 2010). *In vivo*, intestinal uptake of dietary vitamin B_{12} by CUBN occurs independently of megalin (Jensen et al., 2014). However, megalin-dependent internalization of several CUBN ligands has also been reported. For example, transferrin, another CUBN ligand, is internalized by CUBN in a megalin-dependent manner (Kozyraki et al., 2001). Amsellem and colleagues demonstrated that selective inactivation of either megalin or cubilin in mice impedes formation of albumin endocytosed vesicles, and inactivation of both megalin and cubilin did not increase albuminuria, suggesting that the main role of megalin in albumin reabsorption is to drive the internalization of CUBN-albumin complexes (Amsellem et al., 2010). In our cell culture system, we found that CUBN and AMN were sufficient for albumin uptake (Fig. 2; Fig. S2). These seemingly contradictory results could be attributed to a secondary effect of megalin knockout. One of the possibilities is the decreased CUBN expression in the megalin-deficient mouse (Amsellem et al., 2010), which might inhibit megalin-independent CUBAM-mediated endocytosis of albumin. To date, the regulatory mechanisms that control the expression, localization and function of CUBN by megalin have not been well elucidated. Previously, Ahuja and coworkers demonstrated that megalin affects the intracellular turnover of CUBN (Ahuja et al., 2008). The precise function of megalin in the CUBAM-mediated endocytosis of albumin should be examined in future studies.

Although the nucleolus has been classically recognized as a site of RNA polymerase I (RNA Pol I) transcription and ribosome biogenesis, it is now recognized to have multiple significant functions in cellular homeostasis (Nunez Villacis et al., 2018). Most nucleolar proteins are highly dynamic and shuttle between the nucleolus and nucleoplasm, and their translocation regulates DNA repair, RNA Pol II transcription, telomere maintenance, the stress response and apoptosis (Iarovaia et al., 2019). Furthermore, some nucleolar proteins can be trafficked from the nuclei to the extranuclear space. One example is the cyclin-dependent kinase inhibitor p21cip, which transits through the nucleolus on its way from the nucleus to the cytoplasm (Abella et al., 2010; Iarovaia et al., 2019). P21cip has a dual function in oncogenesis, depending mainly on its intracellular localization: p21cip functions as a tumor suppressor in the nucleus and as an oncoprotein in the cytoplasm (Abella et al., 2010). In the present study, NVL translocated from the nucleolus to the extranuclear region in a CUBAM-dependent manner, and extranuclear localization of NVL was confirmed in tissues such as intestine and renal tubules where CUBN and AMN are highly expressed. The finding that NVL2 is involved in albumin uptake reveals a novel nucleolar function in regulating ligand endocytosis mediated by cell surface receptors.

Several studies have reported on NVL in relation to pathological states. Expression of NVL has been found to associate with the invasion and prognosis of prostate cancer (Zhao et al., 2016). The associations of single nucleotide polymorphisms in NVL with psychiatric disorders or diabetic retinopathy have also been reported (Pollack et al., 2019; Wang et al., 2015). However, the functional mechanisms of NVL in the pathogenesis of these diseases are unknown. Genetic animal models of NVL will be required to unravel the differential, and potentially interrelated, roles of NVL in ribosome synthesis, regulation of telomerase activity and endocytosis *in vivo*.

Recent integrative analyses revealed that endolysosomal function in proximal tubular cells is involved in development and progression of chronic kidney disease (Qiu et al., 2018). The receptor-mediated endocytosis of glomerular-filtered toxic substances (Kuwahara et al., 2016) or excessive albumin (Lambers Heerspink and Gansevoort, 2015; Liu et al., 2015) in renal tubular cells exerts cytotoxic effects through a wide array of intracellular signaling pathways. The cellular model described here will help identify the molecular mechanism of albumin endocytosis in physiological and diverse pathologic states.

MATERIALS AND METHODS

Cell lines

HEK293 T (female) and HCT116 (male) cells (ATCC, Manassas, VA, USA) were grown in Dulbecco's modified Eagle's medium (DMEM) with

Journal of Cell Science (2020) 133, jcs242859. doi:10.1242/jcs.242859

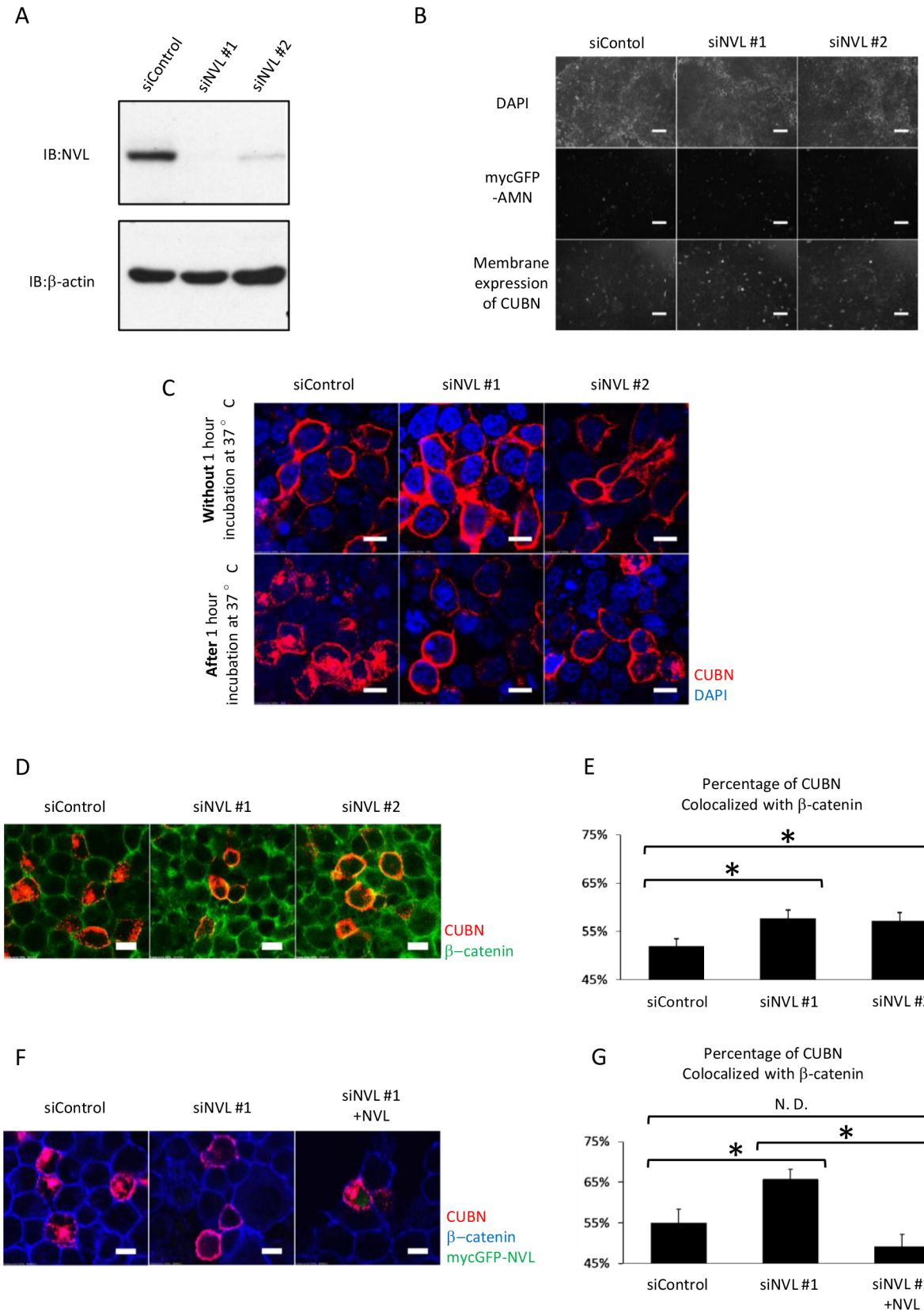

Fig. 6. See next page for legend.

10% fetal bovine serum (FBS) and sodium pyruvate. Flp-In T-REx-293 cells exhibiting doxycycline (Dox)-induced expression of Strep-tagII-tagged NVL2 (wild-type or E365Q/E682Q mutant) were used as described previously (Yoshikatsu et al., 2015). Protein expression was induced by adding 1 g/ml Dox (Sigma-Aldrich, St Louis, MO, USA) 48 h before the experiments. CACO2 (male) cells (ATCC) were grown in DMEM with 10%

Journal of Cell Science (2020) 133, jcs242859. doi:10.1242/jcs.242859

Fig. 6. NVL2 facilitates endocytosis of CUBAM. (A) Expression of NVL2 and β-actin in HEK293T cells transfected with control siRNA (siControl) or NVL siRNA (siNVL #1, siNVL #2). (B) HEK293T cells were transfected with FLAG-tagged mini-CUBN (1-4), myc-tagged AMN and the indicated siRNAs. Membrane expression of CUBN was evaluated by immunofluorescence without permeabilization. (C) The effect of NVL knockdown on CUBN internalization. HEK293T cells were transfected with FLAG-tagged mini-CUBN (1-4), AMN and the indicated siRNAs. CUBN on the cell surface was first labeled with anti-FLAG antibody. The cells were fixed and permeabilized immediately or after incubation at 37°C for 1 h. Cells were stained using secondary antibody conjugated with a fluorescent marker. (D) Co-immunostaining of surface CUBN and β-catenin on the cell membrane after endocytosis in siControl or siNVL cells. HEK293T cells were transfected with FLAG-tagged CUBN, myc-tagged AMN and the indicated siRNAs. (E) Quantification of surface CUBN left on the cell membrane after the endocytosis period. The ratio of CUBN signals colocalized with β-catenin signals to total CUBN signals was calculated using ImageJ. (F) Co-immunostaining of surface CUBN and β-catenin on the cell membrane after endocytosis in siControl cells, siNVL cells or siNVL cells transfected with siRNA-resistant GFP-tagged NVL2. (G) Quantification of surface CUBN left on the cell membrane after the endocytosis period. For E and G, data are shown as mean±s.e.m. (n=10). N.D., no difference, *P<0.05, using a two-sided t-test. Scale bars: 100 µm (B), 10 µm (C,D,F).

FBS, sodium pyruvate and nonessential amino acids (Nacalai Tesque, Japan) on collagen-coated plates. Cells were grown in a humidified atmosphere with 5% CO_2 and 95% air at 37°C. We checked for contamination frequently.

Transfection and RNA interference

Plasmid transfection in HEK293T and Flp-In T-REx-293 cells was performed using PEI-MAX (Polysciences, Warrington, PA, USA) and in HCT116 cells using Lipofectamine 2000 reagent (Invitrogen, Carlsbad, CA, USA). The sequences of siRNAs used were as follows: non-silencing control (Merck, Cat# SIC-001, Kenilworth, NJ, USA), NVL siRNA#1 (5′-CCAGGGAAAGAAUACUUCAAACAUU-3′), NVL siRNA#2 (5′-CAGACCAGUUCAAAGCUCUUGGAUU-3′) and clathrin siRNA (5′-CCGGAAAUUUGAUGUCAAUACUUCA-3′). The siRNA duplexes were transfected into HEK293T and CACO2 cells using Lipofectamine RNAiMAX (Invitrogen) according to the manufacturer's instructions. In some experiments, actinomycin D (final concentration, 5 nM) or CX-5461 (1 µM) was added to the culture medium 3 h or 1 h before the experiment, respectively.

Expression vectors

Full-length cDNA of human NVL1, NVL2, ARH, CUBN and segments comprising the 113 aa N-terminal stretch, EGF repeats and CUB 1-8 domain of CUBN were amplified by PCR and cloned into the pCMV-tag 4A vector (Stratagene, La Jolla, CA, USA). The full-length cDNA of human ARH was amplified by PCR and cloned into pCMV-HA, an HA-tagged vector based on pCMV-tag 4A. To generate pCMV-GFP, eGFP was amplified from a pEGFP-N1 vector using primers with an *Xho*I site in the forward primer and an *Apa*I site and putative splice acceptor site in the reverse primer. pCMV-tag 4A and the amplified eGFP were digested with *Xho*I and *Apa*I. Fragments were ligated to create pCMV-GFP. The pCMV-GFP and FLAG-NVL2 were digested with *Not*I and *Sal*I, and fragments were ligated to create GFP-NVL2. Amplified and digested eGFR fragments were ligated with fragments of FLAG-mini-CUBN (1-4) digested with *Xho*I and *Apa*I to generate GFP-mini-CUBN (1-4). Mutant NVL2 constructs (E365Q, E682Q, K311M and K628M) were generated by PCR-based mutagenesis. siRNA-resistant GFP-NVL2 was generated by introducing silent mutations (5′-ACGTGAGCGGATCTTGCAGACGC-3′) using PCR-based mutagenesis. Myc-DDK-AMN, FLAG-rat-mini-CUBN (1-4) and myc-GFP-AMN were as described (Udagawa et al., 2018). Myc-tagged AMN was generated by inserting a stop codon (TAA) immediately after the myc-tag sequence in the myc-DDK-AMN vector using PCR-based mutagenesis. To generate myc-tagged AMN-ΔICD, the extracellular and transmembrane domain of AMN (1-378 aa) was amplified by PCR and cloned into the pCMV6-Entry vector (OriGene, Rockville, MD, USA) with a stop codon (TAA) inserted immediately after the myc sequence using PCR-based mutagenesis. To generate an *Escherichia coli* expression vector of GST-tagged AMN-ICD and NVL2-NT, the intracellular domain of AMN (379-453 aa) and the N terminus of NVL2 (1-264 aa) were amplified by PCR and cloned into the pGEX-4T-1 vector (GE Healthcare, Buckinghamshire, UK). The myc-tagged, myc-DDK-tagged and myc-GFP-tagged mutant Sdel-AMNs were generated by PCR-based mutagenesis using wild-type myc-AMN, myc-DDK-AMN or myc-GFP-AMN plasmid, respectively. pCMV-tag 4A was used as control empty vector.

Antibodies and reagents

Rabbit polyclonal anti-NVL antibody was affinity-purified from the serum of rabbits that had been injected with recombinant NVL protein (Nagahama et al., 2004). The following antibodies and reagents were obtained from commercial sources: mouse monoclonal anti-DYKDDDDK antibody (Cat# 014-22383, Fujifilm Wako, Japan) used as anti-FLAG antibody for immunoblotting; mouse monoclonal anti-FLAG antibody (Cat# F1804, Merck, Kenilworth, NJ, USA) used as anti-FLAG antibody for assays other than immunoblotting; rat monoclonal anti-HA antibody (Cat# 11867423001, Roche, Basel, Switzerland) used for immunoblotting and immunofluorescence; rabbit polyclonal anti-HA antibody (Cat# 561, Medical & Biological Laboratories, Japan) used for PLA assays; rabbit polyclonal anti-AMN antibody (Cat# HPA000817, Atlas Antibodies, Sweden); mouse monoclonal anti-calnexin antibody (Cat# sc-46669, Santa Cruz, Dallas, TX, USA); mouse monoclonal anti-nucleolin antibody (Cat# sc-17826, Santa Cruz); rabbit polyclonal anti-β-actin antibody (Cat# 4967, Cell Signaling, Danvers, MA, USA); mouse monoclonal anti-β-catenin antibody (Cat# 610154, BD Biosciences, Japan); mouse monoclonal anti-EEA1 antibody (Cat# M176-3, Medical & Biological Laboratories, Japan); anti-FLAG antibody bead (Cat# A2220-5ML, Merck); anti-myc antibody beads (Cat# 016-26503, Fujifilm Wako); anti-HA antibody beads (Cat# 014-23081, Fujifilm Wako); protein G Sepharose (Cat# 17-0618-02, GE Healthcare); glutathione Sepharose (Cat# 17-5132-01, GE Healthcare); FITC-BSA (Cat# A9771-60MG, Merck); actinomycin D (Cat# 00851-44, Nacalai Tesque, Japan); and CX-5461 (Cat# cs-0568, ChemScene, Monmouth Junction, NJ, USA).

Co-immunoprecipitation and western blotting

Co-immunoprecipitation and western blotting were performed as previously described (Udagawa et al., 2018). Cells were lysed for 10 min on ice in a lysis buffer (20 mM Tris-HCl pH 7.5, 150 mM NaCl, 1 mM EDTA and 1% NP-40) containing a protease inhibitor cocktail (Nacalai Tesque, Japan). Lysates were clarified by centrifugation and incubated with agarose beads conjugated with anti-FLAG antibody, anti-myc antibody or anti-HA antibody for 1 h at 4°C. For immunoprecipitation with anti-AMN antibody, lysates were incubated with protein G Sepharose for 1 h at 4°C. After centrifugation, the supernatants were collected and incubated with anti-AMN antibody for 1 h at 4°C and then incubated with protein G Sepharose beads for another 1 h at 4°C. For immunoprecipitation of cell surface CUBN, cells were incubated in medium containing anti-FLAG antibody (1:1000) on ice for 1 h to label FLAG-mini-CUBN on the cell surface, and lysates were incubated with protein G Sepharose for 1 h at 4°C. Beads were washed three times with lysis buffer and bound proteins were eluted with SDS sample buffer.

Cell lysates were separated by SDS-PAGE and transferred to polyvinylidene difluoride membranes. Membranes were probed by the appropriate primary antibody; horseradish peroxidase-conjugated anti-mouse IgG, anti-rabbit IgG (GE Healthcare, Buckinghamshire, UK) or anti rat-IgG (abcam, Cambridge, UK) was used as secondary antibody. Peroxidase activity was detected using the ECL or ECL-Plus system (GE Healthcare).

Immunofluorescence

Immunofluorescence staining was performed as previously described (Udagawa et al., 2018). HEK293T cells were cultured on glass slides in 24-well plates (Falcon; BD Biosciences, San Jose, CA, USA) under the conditions described above. For analysis of surface expression of CUBN in

Journal of Cell Science (2020) 133, jcs242859. doi:10.1242/jcs.242859

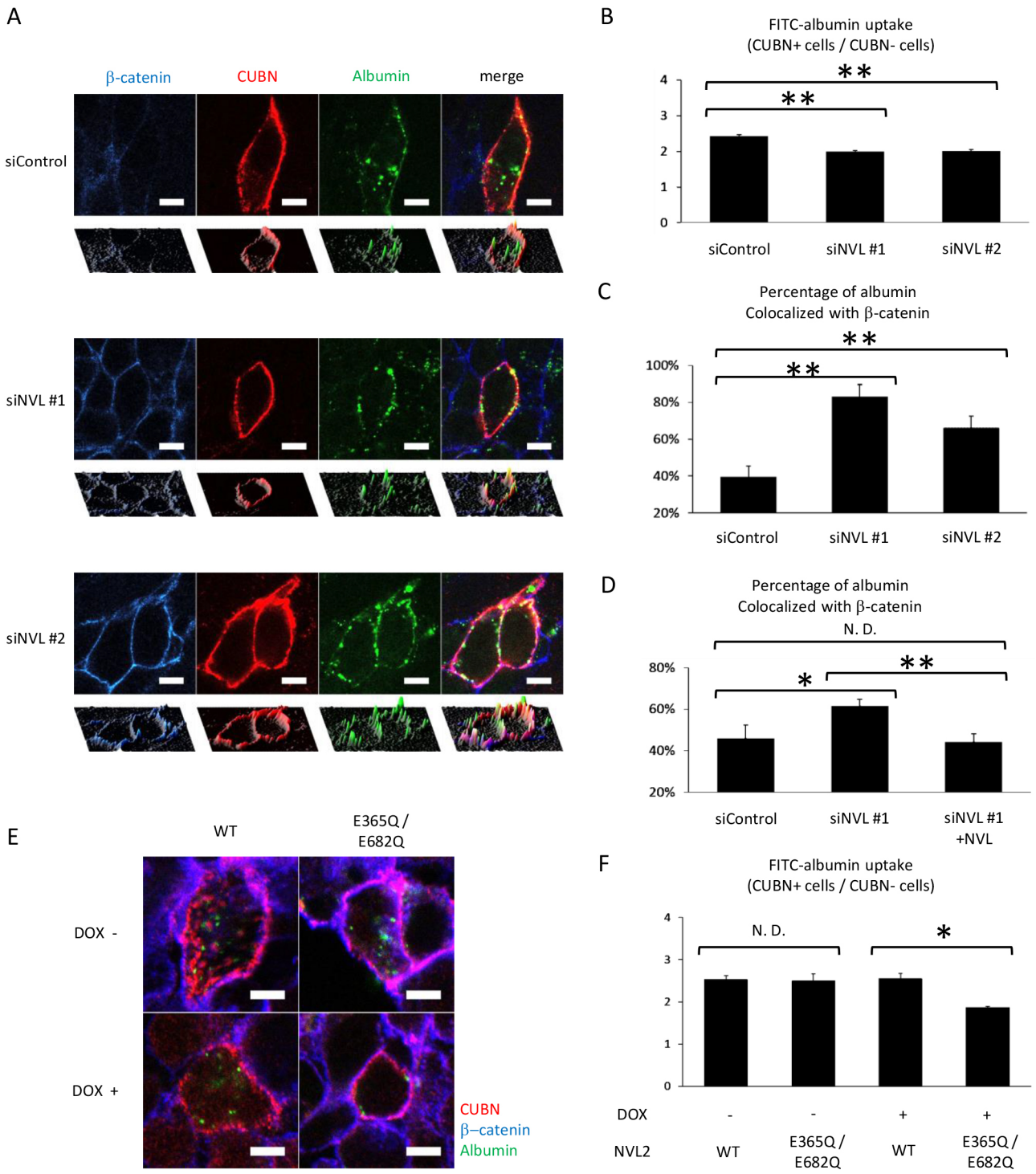

Fig. 7. NVL2 facilitates albumin uptake by CUBN. (A) FITC-albumin uptake by HEK293T cells expressing full-length CUBN with AMN and transfected with the indicated siRNAs. Cells were immunostained for β-catenin and surface FLAG-tagged CUBN after FITC-albumin uptake. (B) Flow cytometric quantification of FITC-albumin uptake in HEK293T cells with control or NVL knockdown performed as for Fig. 1E (n=3). (C,D) Quantification of FITC-albumin retained on the cell membrane. HEK293T cells were transfected with FLAG-tagged CUBN, myc-tagged AMN and the indicated siRNAs. In the indicated sample in D, siRNA-resistant NVL2 was also transfected. Cells were immunostained for β-catenin and surface FLAG-tagged CUBN after FITC-albumin uptake. The ratio of FITC-albumin signals colocalized with β-catenin signals to total FITC-albumin signals was calculated using ImageJ (n=10). (E) FITC-albumin uptake by cells transfected with full-length CUBN and AMN in which NVL2 (wild-type or E365Q/E682Q) was expressed in a Dox-inducible manner. Cells were immunostained for β-catenin and surface FLAG-tagged CUBN after FITC-albumin uptake. (F) Flow cytometric quantification of FITC-albumin uptake in Dox-inducible NVL2-expressing cells in E (n=3). All data are shown as mean±s.e.m. N.D., no difference, *P<0.05, **P<0.01 using a two-sided t-test. Scale bars: 5 µm.

nonpermeabilized samples, cells were fixed with 2% paraformaldehyde in phosphate-buffered saline (PBS) for 5 min. For analysis of protein expression in permeabilized samples, cells were fixed with 3.7% formaldehyde in PBS for 10 min and permeabilized by 0.1% Triton X-100 in PBS for 10 min. Cells were incubated with 1% BSA in PBS for 30 min, followed by incubation with primary antibody for 1 h. Antibodies

Journal of Cell Science (2020) 133, jcs242859. doi:10.1242/jcs.242859

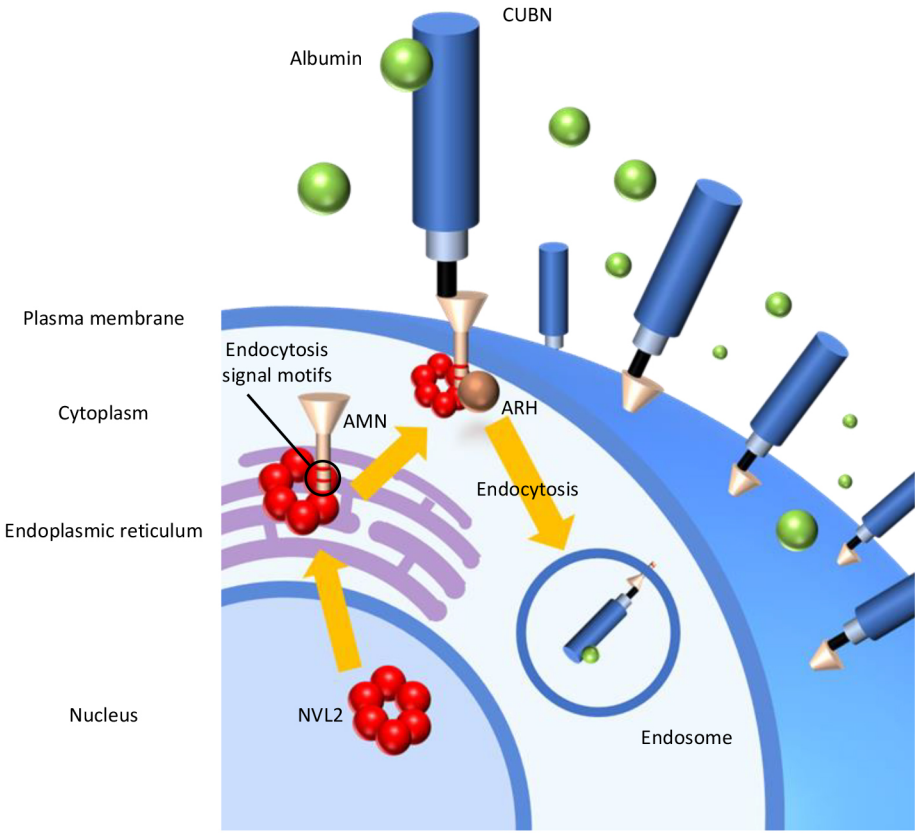

Fig. 8. Model of CUBAM-mediated albumin endocytosis regulated by NVL2. NVL2 translocates from the nucleus to the extranuclear compartment through interaction with the intracellular domain of AMN. NVL2 facilitates CUBAM-mediated endocytosis of albumin.

conjugated with Alexa Fluor 488, 555 or 647 (Invitrogen, Carlsbad, CA, USA) were used as secondary detection antibodies. Slides were mounted in a medium with DAPI (Life Technologies, Carlsbad, CA, USA). Stained cells were visualized using a confocal microscope (LV300; Olympus, Tokyo, Japan) or a fluorescence microscope (IX71; Olympus, Tokyo, Japan). Images were processed using ImageJ (National Institutes of Health, Bethesda, MD, USA). The 3D surface plots in Fig. 1G, Fig. 4C,D and Fig. 7A were generated using ImageJ.

FITC-BSA endocytosis assay

HEK293T cells expressing FLAG-CUBN [mini-CUBN (1-4), miniCUBN(1-8) or full-length CUBN] and myc-AMN (wild-type or Sdel) were incubated in medium containing FITC-BSA (100 ng/ml) for 1 h at 37°C. To label FLAG-CUBN on the cell surface, cells were incubated in medium containing anti-FLAG antibody (1:1000) for 1 h on ice. Cells were fixed, permeabilized and stained with the secondary antibody [anti-mouse IgG antibody with Alexa Fluor 555 for microscopy or anti-mouse IgG antibody with Alexa Fluor 647 for flow cytometry (Invitrogen)]. Endogenous β-catenin was also stained with anti-β-catenin antibody conjugated with Alexa Fluor 647 using the Zenon Antibody Labeling Kit (Thermo Fisher Scientific, Waltham, MA, USA).

CACO2 cells were incubated in medium containing FITC-BSA (100 ng/ml) for 1 h at 37°C. Cells were immediately fixed and permeabilized. Cells were also stained with anti-β-catenin antibody, followed by staining with the secondary antibody (anti-mouse IgG antibody with Alexa Fluor 555).

Flow cytometry

FITC-BSA uptake and surface CUBN staining were performed as described above. Cell gating and data collecting were performed with FACS Gallios (Beckman Coulter Life Sciences, Brea, CA, USA). Data were analyzed using Kaluza (Beckman Coulter Life Sciences).

SILAC labeling and mass spectrometry analysis

SILAC labeling and mass spectrometry analyses were performed as previously described (Udagawa et al., 2018). Briefly, HEK293T cells cultured in medium containing amino acids labeled with heavy isotopes (L-$^{13}C_6^{15}N_4$-Arg and L-$^{13}C_6$-Lys) were transfected with myc-DDK-AMN and cells in 'light' medium (with L-$^{12}C_6^{14}N_4$-Arg and L-$^{12}C_6$-Lys) were transfected with empty vector. Cell lysates were mixed and immunoprecipitated. After enzymatic digestion of protein samples, mass spectrometry analysis was carried out using data-dependent MS/MS with a Q-FT mass spectrometer (Q-Exactive, Thermo Fisher Scientific) equipped with a nano-HPLC system (Advance UHPLC, Bruker Daltonics) and an HTC-PAL autosampler (CTC Analytics) with a trap column (0.3×5 mm; L-column ODS, Chemicals Evaluation and Research Institute, Japan). The peptides and proteins were identified and quantified using Proteome Discoverer 1.4 software (Thermo Fisher Scientific) with the SequestHT algorithm.

Proximity ligation assay

Proximity ligation assay (PLA) was performed using the Duolink *in situ* PLA kit (Olink Bioscience, Sweden) as described previously (Tsurumi et al., 2016). HEK293T cells were cultured on coverslips coated with collagen type 1, fixed and permeabilized. After washing in PBS, cells were blocked in blocking solution (1% BSA in PBS) for 30 min. After washing, samples were incubated for 1 h at 37°C with diluted primary antibodies (mouse anti-FLAG antibody and rabbit anti-AMN antibody for FLAG-NVL2 and myc- or mycGFP-AMN; mouse anti-FLAG antibody and rabbit anti-HA antibody for FLAG-ARH and HA-NVL2), followed by incubation for 1 h at 37°C with the corresponding secondary antibodies conjugated to PLA oligonucleotide probes (Duolink PLA Rabbit PLUS and PLA Mouse MINUS proximity probes). Hybridization and ligation of connector oligonucleotides, rolling-circle amplification and detection of amplified DNA products using detection reagent Red were performed using the Duolink detection reagent kit according to the manufacturer's protocol. In the indicated samples, additional immunofluorescence staining for endogenous CNX or β-catenin was performed after the PLA assay. Samples were stained with DAPI before mounting.

Immunohistological analyses

Human kidney and intestine samples were obtained commercially (Cosmo Bio, Japan). Immunohistological analyses were performed as previously described (Udagawa et al., 2018). Paraffin-embedded samples were deparaffinized in xylene and rehydrated through a series of graded alcohols in H_2O, followed by heat-induced epitope retrieval by incubating in a target retrieval solution (S1699; Dako, Carpinteria, CA, USA) for 20 min at 121°C. Sections were cooled to room temperature and incubated with primary antibodies, followed by incubation with secondary antibodies (Invitrogen). For co-immunostaining of AMN and NVL, samples were first stained with NVL as described, followed by staining with anti-AMN antibody with Alexa Fluor 555 conjugated using the Zenon Antibody Labeling Kit (Thermo Fisher Scientific) and subsequent fixation with 3.7% formaldehyde in PBS. Confocal fluorescent images were obtained using an Olympus LV300 confocal microscope. Images were processed using ImageJ.

In vitro pull-down assay

GST, GST-fused AMN-ICD and GST-fused NVL2-NT peptides were expressed in BL21 *E. coli*. Cells were precipitated by centrifugation, lysed in sonication buffer (1 mM dithiothreitol, 1% NP-40 in Tris-HCl-buffered saline) containing protease inhibitor cocktail (Nacalai Tesque, Japan) and sonicated (30 s×4 sets) on ice. Lysates were clarified by centrifugation and incubated with glutathione Sepharose beads for 1 h at 4°C. Beads were washed twice with washing buffer (1% NP-40 in TBS) containing 0.5 mM NaCl, washed three times with washing buffer and then incubated for 1 h at 4°C with lysates of HEK293T cells expressing FLAG-NVL2 or myc-DDK-AMN. After three washes with washing buffer, bound proteins were eluted with SDS sample buffer and analyzed by western blotting.

Endocytosis assay

HEK293T and HCT116 cells expressing FLAG-tagged mini-CUBN (1-4) and myc-tagged AMN were incubated in medium containing anti-FLAG antibody (1:1000) on ice for 1 h to label FLAG-mini-CUBN on the cell surface. For analysis of CUBN localization before the internalization period, cells were immediately fixed, permeabilized and stained with the secondary antibody (anti-mouse IgG antibody conjugated with Alexa Fluor 555). For analysis of CUBN localization after the internalization period, cells were incubated in PBS for 1 h at 37°C, fixed, permeabilized and stained with secondary antibody. In indicated samples, cells were also stained for endogenous β-catenin with anti-β-catenin antibody with the Alexa Fluor 488 or 647 conjugated using the Zenon Antibody Labeling Kit (Thermo Fisher Scientific). Slides were mounted in medium with DAPI (Life Technologies). Stained cells were visualized using a confocal microscope (LV300; Olympus, Tokyo, Japan). Images were processed and analyzed using ImageJ.

Pre-absorption of anti-NVL antibody

Immunoprecipitation was performed using anti-FLAG antibodies in lysates of HEK293T cells expressing FLAG-tagged control protein (FLAG-KLHL3) or FLAG-NVL2. Diluted NVL primary antibody was incubated overnight with the immunoprecipitates at 4°C.

Quantitative PCR

mRNAs were extracted from cells using ISOGEN-LS (Nippon Gene, Tokyo, Japan) and reverse transcribed into cDNAs using SuperScript III Reverse Transcriptase (Thermo Fisher Scientific). Quantitative PCR was performed with 400 ng of cDNAs, primer sets (5′-AACTGGAGCCAGAACCGGAC-3′ and 5′-AGGAGGCACTAGGCGGAAAG-3′ for AMN, 5′-TTCACTGCCG-TCTTCCAGTC-3′ and 5′-CACAGCGGAACGAGCTTCTA-3′ for CUBN, and 5′-TGCACCACCAACTGCTTAGC-3′ and 5′-GGCATGGACTGTGGT-CATGAG-3′ for GAPDH) and THUNDERBIRD SYBR qPCR Mix (Toyobo, Osaka, Japan). Amplification was run in a CFX Connect thermal cycler (BioRad, Hercules, CA, USA) at 95°C for 3 min followed by 40 cycles of 95°C for 15 s and 60°C for 1 min. Melting curve analysis was performed by heating the reactions from 65 to 95°C in 0.5°C intervals while monitoring fluorescence. Data were analyzed with Bio-Rad CFX manager 3.1 (BioRad).

Statistical analysis

ImageJ was used to quantify area size. Results are presented as mean± standard error of the mean (s.e.m.). The numbers of samples is given in the figure legends. Significant differences between means of two sample groups were evaluated using a two-sided *t*-test, with significance indicated for $P<0.05$.

Acknowledgements

We appreciate Dr Yasuhiro Yoshida, Department of Pediatrics, Graduate School of Medicine, University of Tokyo, for constructing the FLAG-NVL2 expression vector. We thank Life Sciences Core Facility, Graduate School of Medicine, University of Tokyo for supporting the flow cytometry analysis. We thank Edanz Group (www.edanzediting.com/ac) for editing a draft of the manuscript.

Competing interests

The authors declare no competing or financial interests.

Author contributions

Conceptualization: S.U., Y.H., M. Nagahama, Y.K., S.K.; Methodology: S.U., Y.H., T.U., M. Nagahama, H.R.U., M. Nangaku; Software: S.U., K.L.O.; Validation: S.U., Y.H.; Formal analysis: S.U., Y.H., K.L.O.; Investigation: S.U.; Resources: S.U., Y.H., T.U., M. Nagahama, A.S., M. Nangaku; Data curation: S.U., T.U., K.L.O., H.R.U.; Writing - original draft: S.U., Y.H.; Writing - review & editing: S.U., Y.H., T.U., K.L.O., M. Nagahama, Y.K., S.K., A.S., H.R.U., M. Nangaku, A.O.; Visualization: S.U.; Supervision: S.U., Y.H., Y.K., S.K., H.R.U., M. Nangaku, A.O.; Project administration: S.U., Y.H.; Funding acquisition: S.U., Y.H.

Funding

This work is supported in part by a Grant-in-Aid for Japan Society for the Promotion of Science (JSPS) Research Fellow (18J12813 to S.U.), and a Grant-in-Aid from the Ministry of Education, Culture, Sports, Science and Technology of Japan for Scientific Research (C) (18K07872 to Y.H.).

Supplementary information

Supplementary information available online at https://jcs.biologists.org/lookup/doi/10.1242/jcs.242859.supplemental

Peer review history

The peer review history is available online at https://jcs.biologists.org/lookup/doi/10.1242/jcs.242859.reviewer-comments.pdf

References

Abella, N., Brun, S., Calvo, M., Tapia, O., Weber, J. D., Berciano, M. T., Lafarga, M., Bachs, O. and Agell, N. (2010). Nucleolar disruption ensures nuclear accumulation of p21 upon DNA damage. *Traffic* **11**, 743-755. doi:10.1111/j.1600-0854.2010.01063.x

Ahluwalia, T. S., Schulz, C. A., Waage, J., Skaaby, T., Sandholm, N., van Zuydam, N., Charmet, R., Bork-Jensen, J., Almgren, P., Thuesen, B. H. et al. (2019). A novel rare CUBN variant and three additional genes identified in Europeans with and without diabetes: results from an exome-wide association study of albuminuria. *Diabetologia* **62**, 292-305. doi:10.1007/s00125-018-4783-z

Ahuja, R., Yammani, R., Bauer, J. A., Kalra, S., Seetharam, S. and Seetharam, B. (2008). Interactions of cubilin with megalin and the product of the amnionless gene (AMN): effect on its stability. *Biochem. J.* **410**, 301-308. doi:10.1042/BJ20070919

Aminoff, M., Carter, J. E., Chadwick, R. B., Johnson, C., Gräsbeck, R., Abdelaal, M. A., Broch, H., Jenner, L. B., Verroust, P. J., Moestrup, S. K. et al. (1999). Mutations in CUBN, encoding the intrinsic factor-vitamin B12 receptor, cubilin, cause hereditary megaloblastic anaemia 1. *Nat. Genet.* **21**, 309-313. doi:10.1038/6831

Amsellem, S., Gburek, J., Hamard, G., Nielsen, R., Willnow, T. E., Devuyst, O., Nexo, E., Verroust, P. J., Christensen, E. I. and Kozyraki, R. (2010). Cubilin is essential for albumin reabsorption in the renal proximal tubule. *J. Am. Soc. Nephrol.* **21**, 1859-1867. doi:10.1681/ASN.2010050492

Andersen, C. B. F., Madsen, M., Storm, T., Moestrup, S. K. and Andersen, G. R. (2010). Structural basis for receptor recognition of vitamin-B(12)-intrinsic factor complexes. *Nature* **464**, 445-448. doi:10.1038/nature08874

Batuman, V., Verroust, P. J., Navar, G. L., Kaysen, J. H., Goda, F. O., Campbell, W. C., Simon, E., Pontillon, F., Lyles, M., Bruno, J. et al. (1998). Myeloma light chains are ligands for cubilin (gp280). *Am. J. Physiol.* **275**, F246-F254. doi:10.1152/ajprenal.1998.275.2.F246

Bedin, M., Boyer, O., Servais, A., Li, Y., Villoing-Gaudé, L., Tête, M.-J., Cambier, A., Hogan, J., Baudouin, V., Krid, S. et al. (2020). Human C-terminal CUBN variants associate with chronic proteinuria and normal renal function. *J. Clin. Invest.* **130**, 335-344. doi:10.1172/JCI129937

Birn, H. and Christensen, E. I. (2006). Renal albumin absorption in physiology and pathology. *Kidney Int.* **69**, 440-449. doi:10.1038/sj.ki.5000141

Birn, H., Fyfe, J. C., Jacobsen, C., Mounier, F., Verroust, P. J., Ørskov, H., Willnow, T. E., Moestrup, S. K. and Christensen, E. I. (2000). Cubilin is an albumin binding protein important for renal tubular albumin reabsorption. *J. Clin. Invest.* **105**, 1353-1361. doi:10.1172/JCI8862

Birn, H., Verroust, P. J., Nexø, E., Hager, H., Jacobsen, C., Christensen, E. I. and Moestrup, S. K. (1997). Characterization of an epithelial approximately 460-kDa protein that facilitates endocytosis of intrinsic factor-vitamin B12 and binds receptor-associated protein. *J. Biol. Chem.* **272**, 26497-26504. doi:10.1074/jbc.272.42.26497

Boger, C. A., Chen, M.-H., Tin, A., Olden, M., Köttgen, A., de Boer, I. H., Fuchsberger, C., O'Seaghdha, C. M., Pattaro, C., Teumer, A. et al. (2011). CUBN is a gene locus for albuminuria. *J. Am. Soc. Nephrol.* **22**, 555-570. doi:10.1681/ASN.2010060598

Boulon, S., Westman, B. J., Hutten, S., Boisvert, F.-M. and Lamond, A. I. (2010). The nucleolus under stress. *Mol. Cell* **40**, 216-227. doi:10.1016/j.molcel.2010.09.024

Carmo-Fonseca, M., Pepperkok, R., Carvalho, M. T. and Lamond, A. I. (1992). Transcription-dependent colocalization of the U1, U2, U4/U6, and U5 snRNPs in coiled bodies. *J. Cell Biol.* **117**, 1-14. doi:10.1083/jcb.117.1.1

Christensen, E. I., Nielsen, R. and Birn, H. (2013). From bowel to kidneys: the role of cubilin in physiology and disease. *Nephrol. Dial. Transplant.* **28**, 274-281. doi:10.1093/ndt/gfs565

Comper, W. D., Hilliard, L. M., Nikolic-Paterson, D. J. and Russo, L. M. (2008). Disease-dependent mechanisms of albuminuria. *Am. J. Physiol. Renal. Physiol.* **295**, F1589-F1600. doi:10.1152/ajprenal.00142.2008

Coudroy, G., Gburek, J., Kozyraki, R., Madsen, M., Trugnan, G., Moestrup, S. K., Verroust, P. J. and Maurice, M. (2005). Contribution of cubilin and amnionless to processing and membrane targeting of cubilin-amnionless complex. *J. Am. Soc. Nephrol.* **16**, 2330-2337. doi:10.1681/ASN.2004110925

Drygin, D., Lin, A., Bliesath, J., Ho, C. B., O'Brien, S. E., Proffitt, C., Omori, M., Haddach, M., Schwaebe, M. K., Siddiqui-Jain, A. et al. (2011). Targeting RNA polymerase I with an oral small molecule CX-5461 inhibits ribosomal RNA synthesis and solid tumor growth. *Cancer Res.* **71**, 1418-1430. doi:10.1158/0008-5472.CAN-10-1728

Eshbach, M. L. and Weisz, O. A. (2017). Receptor-mediated endocytosis in the proximal tubule. *Annu. Rev. Physiol.* **79**, 425-448. doi:10.1146/annurev-physiol-022516-034234

Fanali, G., di Masi, A., Trezza, V., Marino, M., Fasano, M. and Ascenzi, P. (2012). Human serum albumin: from bench to bedside. *Mol. Aspects Med.* **33**, 209-290. doi:10.1016/j.mam.2011.12.002

Fyfe, J. C., Ramanujam, K. S., Ramaswamy, K., Patterson, D. F. and Seetharam, B. (1991). Defective brush-border expression of intrinsic factor-cobalamin receptor in canine inherited intestinal cobalamin malabsorption. *J. Biol. Chem.* **266**, 4489-4494.

Fyfe, J. C., Madsen, M., Højrup, P., Christensen, E. I., Tanner, S. M., de la Chapelle, A., He, Q. and Moestrup, S. K. (2004). The functional cobalamin (vitamin B12)-intrinsic factor receptor is a novel complex of cubilin and amnionless. *Blood* **103**, 1573-1579. doi:10.1182/blood-2003-08-2852

Gburek, J., Verroust, P. J., Willnow, T. E., Fyfe, J. C., Nowacki, W., Jacobsen, C., Moestrup, S. K. and Christensen, E. I. (2002). Megalin and cubilin are endocytic receptors involved in renal clearance of hemoglobin. *J. Am. Soc. Nephrol.* **13**, 423-430.

Gekle, M. (2005). Renal tubule albumin transport. *Annu. Rev. Physiol.* **67**, 573-594. doi:10.1146/annurev.physiol.67.031103.154845

Germain-Lee, E. L., Obie, C. and Valle, D. (1997). NVL: a new member of the AAA family of ATPases localized to the nucleus. *Genomics* **44**, 22-34. doi:10.1006/geno.1997.4856

Gianesello, L., Priante, G., Ceol, M., Radu, C. M., Saleem, M. A., Simioni, P., Terrin, L., Anglani, F. and Del Prete, D. (2017). Albumin uptake in human podocytes: a possible role for the cubilin-amnionless (CUBAM) complex. *Sci. Rep.* **7**, 13705. doi:10.1038/s41598-017-13789-z

Gräsbeck, R. (2006). Imerslund-Grasbeck syndrome (selective vitamin B(12) malabsorption with proteinuria). *Orphanet J. Rare Dis.* **1**, 17. doi:10.1186/1750-1172-1-17

Haas, M. E., Aragam, K. G., Emdin, C. A., Bick, A. G., Hemani, G., Davey Smith, G. and Kathiresan, S. (2018). Genetic association of albuminuria with cardiometabolic disease and blood pressure. *Am. J. Hum. Genet.* **103**, 461-473. doi:10.1016/j.ajhg.2018.08.004

Hammad, S. M., Barth, J. L., Knaak, C. and Argraves, W. S. (2000). Megalin acts in concert with cubilin to mediate endocytosis of high density lipoproteins. *J. Biol. Chem.* **275**, 12003-12008. doi:10.1074/jbc.275.16.12003

He, Q., Madsen, M., Kilkenney, A., Gregory, B., Christensen, E. I., Vorum, H., Hojrup, P., Schaffer, A. A., Kirkness, E. F., Tanner, S. M. et al. (2005). Amnionless function is required for cubilin brush-border expression and intrinsic factor-cobalamin (vitamin B12) absorption in vivo. *Blood* **106**, 1447-1453. doi:10.1182/blood-2005-03-1197

Her, J. and Chung, I. K. (2012). The AAA-ATPase NVL2 is a telomerase component essential for holoenzyme assembly. *Biochem. Biophys. Res. Commun.* **417**, 1086-1092. doi:10.1016/j.bbrc.2011.12.101

Iarovaia, O. V., Minina, E. P., Sheval, E. V., Onichtchouk, D., Dokudovskaya, S., Razin, S. V. and Vassetzky, Y. S. (2019). Nucleolus: a central hub for nuclear functions. *Trends Cell Biol.* **29**, 647-659. doi:10.1016/j.tcb.2019.04.003

Jensen, L. L., Andersen, R. K., Hager, H. and Madsen, M. (2014). Lack of megalin expression in adult human terminal ileum suggests megalin-independent cubilin/amnionless activity during vitamin B12 absorption. *Physiol. Rep.* **2**, e12086. doi:10.14814/phy2.12086

Kalantry, S., Manning, S., Haub, O., Tomihara-Newberger, C., Lee, H.-G., Fangman, J., Disteche, C. M., Manova, K. and Lacy, E. (2001). The amnionless gene, essential for mouse gastrulation, encodes a visceral-endoderm-specific protein with an extracellular cysteine-rich domain. *Nat. Genet.* **27**, 412-416. doi:10.1038/86912

Kozyraki, R., Kristiansen, M., Silahtaroglu, A., Hansen, C., Jacobsen, C., Tommerup, N., Verroust, P. J. and Moestrup, S. K. (1998). The human intrinsic factor-vitamin B12 receptor, cubilin: molecular characterization and chromosomal mapping of the gene to 10p within the autosomal recessive megaloblastic anemia (MGA1) region. *Blood* **91**, 3593-3600. doi:10.1182/blood.V91.10.3593

Kozyraki, R., Fyfe, J., Kristiansen, M., Gerdes, C., Jacobsen, C., Cui, S., Christensen, E. I., Aminoff, M., de la Chapelle, A., Krahe, R. et al. (1999). The intrinsic factor-vitamin B12 receptor, cubilin, is a high-affinity apolipoprotein A-I receptor facilitating endocytosis of high-density lipoprotein. *Nat. Med.* **5**, 656-661. doi:10.1038/9504

Kozyraki, R., Fyfe, J., Verroust, P. J., Jacobsen, C., Dautry-Varsat, A., Gburek, J., Willnow, T. E., Christensen, E. I. and Moestrup, S. K. (2001). Megalin-dependent cubilin-mediated endocytosis is a major pathway for the apical uptake of transferrin in polarized epithelia. *Proc. Natl. Acad. Sci. USA* **98**, 12491-12496. doi:10.1073/pnas.211291398

Kuwahara, S., Hosojima, M., Kaneko, R., Aoki, H., Nakano, D., Sasagawa, T., Kabasawa, H., Kaseda, R., Yasukawa, R., Ishikawa, T. et al. (2016). Megalin-mediated tubuloglomerular alterations in high-fat diet-induced kidney disease. *J. Am. Soc. Nephrol.* **27**, 1996-2008. doi:10.1681/ASN.2015020190

Lambers Heerspink, H. J. and Gansevoort, R. T. (2015). Albuminuria is an appropriate therapeutic target in patients with CKD: the pro view. *Clin. J. Am. Soc. Nephrol.* **10**, 1079-1088. doi:10.2215/CJN.11511114

Liu, D., Wen, Y., Tang, T.-T., Lv, L.-L., Tang, R.-N., Liu, H., Ma, K.-L., Crowley, S. D. and Liu, B.-C. (2015). Megalin/cubulin-lysosome-mediated albumin reabsorption is involved in the tubular cell activation of NLRP3 Inflammasome and tubulointerstitial inflammation. *J. Biol. Chem.* **290**, 18018-18028. doi:10.1074/jbc.M115.662064

Lo, Y.-H., Sobhany, M., Hsu, A. L., Ford, B. L., Krahn, J. M., Borgnia, M. J. and Stanley, R. E. (2019). Cryo-EM structure of the essential ribosome assembly AAA-ATPase Rix7. *Nat. Commun.* **10**, 513. doi:10.1038/s41467-019-08373-0

Moestrup, S. K., Kozyraki, R., Kristiansen, M., Kaysen, J. H., Rasmussen, H. H., Brault, D., Pontillon, F., Goda, F. O., Christensen, E. I., Hammond, T. G. et al. (1998). The intrinsic factor-vitamin B12 receptor and target of teratogenic antibodies is a megalin-binding peripheral membrane protein with homology to developmental proteins. *J. Biol. Chem.* **273**, 5235-5242. doi:10.1074/jbc.273.9.5235

Mu, F. T., Callaghan, J. M., Steele-Mortimer, O., Stenmark, H., Parton, R. G., Campbell, P. L., McCluskey, J., Yeo, J. P., Tock, E. P. and Toh, B. H. (1995). EEA1, an early endosome-associated protein. EEA1 is a conserved alpha-helical peripheral membrane protein flanked by cysteine "fingers" and contains a calmodulin-binding IQ motif. *J. Biol. Chem.* **270**, 13503-13511. doi:10.1074/jbc.270.22.13503

Nagahama, M., Hara, Y., Seki, A., Yamazoe, T., Kawate, Y., Shinohara, T., Hatsuzawa, K., Tani, K. and Tagaya, M. (2004). NVL2 is a nucleolar AAA-ATPase that interacts with ribosomal protein L5 through its nucleolar localization sequence. *Mol. Biol. Cell* **15**, 5712-5723. doi:10.1091/mbc.e04-08-0692

Nagahama, M., Yamazoe, T., Hara, Y., Tani, K., Tsuji, A. and Tagaya, M. (2006). The AAA-ATPase NVL2 is a component of pre-ribosomal particles that interacts with the DExD/H-box RNA helicase DOB1. *Biochem. Biophys. Res. Commun.* **346**, 1075-1082. doi:10.1016/j.bbrc.2006.06.017

Nagai, J., Sato, K., Yumoto, R. and Takano, M. (2011). Megalin/cubilin-mediated uptake of FITC-labeled IgG by OK kidney epithelial cells. *Drug Metab. Pharmacokinet* **26**, 474-485. doi:10.2133/dmpk.DMPK-11-RG-022

Naldi, M., Baldassarre, M., Domenicali, M., Bartolini, M. and Caraceni, P. (2017). Structural and functional integrity of human serum albumin: Analytical approaches and clinical relevance in patients with liver cirrhosis. *J. Pharm. Biomed. Anal.* **144**, 138-153. doi:10.1016/j.jpba.2017.04.023

Nielsen, R., Christensen, E. I. and Birn, H. (2016). Megalin and cubilin in proximal tubule protein reabsorption: from experimental models to human disease. *Kidney Int.* **89**, 58-67. doi:10.1016/j.kint.2015.11.007

Nunez Villacis, L., Wong, M. S., Ferguson, L. L., Hein, N., George, A. J. and Hannan, K. M. (2018). New roles for the nucleolus in health and disease. *BioEssays* **40**, e1700233. doi:10.1002/bies.201700233

Ovunc, B., Otto, E. A., Vega-Warner, V., Saisawat, P., Ashraf, S., Ramaswami, G., Fathy, H. M., Schoeb, D., Chernin, G., Lyons, R. H. et al. (2011). Exome sequencing reveals cubilin mutation as a single-gene cause of proteinuria. *J. Am. Soc. Nephrol.* **22**, 1815-1820. doi:10.1681/ASN.2011040337

Ozawa, M., Baribault, H. and Kemler, R. (1989). The cytoplasmic domain of the cell adhesion molecule uvomorulin associates with three independent proteins structurally related in different species. *EMBO J.* **8**, 1711-1717. doi:10.1002/j.1460-2075.1989.tb03563.x

Parving, H.-H., Persson, F. and Rossing, P. (2015). Microalbuminuria: a parameter that has changed diabetes care. *Diabetes Res. Clin. Pract.* **107**, 1-8. doi:10.1016/j.diabres.2014.10.014

Pedersen, G. A., Chakraborty, S., Steinhauser, A. L., Traub, L. M. and Madsen, M. (2010). AMN directs endocytosis of the intrinsic factor-vitamin B(12) receptor cubam by engaging ARH or Dab2. *Traffic* **11**, 706-720. doi:10.1111/j.1600-0854.2010.01042.x

Pollock, C. A. and Poronnik, P. (2007). Albumin transport and processing by the proximal tubule: physiology and pathophysiology. *Curr. Opin Nephrol. Hypertens.* **16**, 359-364. doi:10.1097/MNH.0b013e3281eb9059

Pollack, S., Igo, R. P., Jr, Jensen, R. A., Christiansen, M., Li, X., Cheng, C.-Y., Ng, M. C. Y., Smith, A. V., Rossin, E. J., Segre, A. V. et al. (2019). Multiethnic genome-wide association study of diabetic retinopathy using liability threshold modeling of duration of diabetes and glycemic control. *Diabetes* **68**, 441-456. doi:10.2337/db18-0567

Qiu, C., Huang, S., Park, J., Park, Y., Ko, Y.-A., Seasock, M. J., Bryer, J. S., Xu, X. X., Song, W. C., Palmer, M. et al. (2018). Renal compartment-specific genetic variation analyses identify new pathways in chronic kidney disease. *Nat. Med.* **24**, 1721-1731. doi:10.1038/s41591-018-0194-4

Quinlan, G. J., Martin, G. S. and Evans, T. W. (2005). Albumin: biochemical properties and therapeutic potential. *Hepatology* **41**, 1211-1219. doi:10.1002/hep.20720

Saito, A., Pietromonaco, S., Loo, A. K. and Farquhar, M. G. (1994). Complete cloning and sequencing of rat gp330/"megalin," a distinctive member of the low density lipoprotein receptor gene family. *Proc. Natl. Acad. Sci. USA* **91**, 9725-9729. doi:10.1073/pnas.91.21.9725

Spinella, R., Sawhney, R. and Jalan, R. (2016). Albumin in chronic liver disease: structure, functions and therapeutic implications. *Hepatol. Int.* **10**, 124-132. doi:10.1007/s12072-015-9665-6

Storm, T., Emma, F., Verroust, P. J., Hertz, J. M., Nielsen, R. and Christensen, E. I. (2011). A patient with cubilin deficiency. *N. Engl. J. Med.* **364**, 89-91. doi:10.1056/NEJMc1009804

Strope, S., Rivi, R., Metzger, T., Manova, K. and Lacy, E. (2004). Mouse amnionless, which is required for primitive streak assembly, mediates cell-surface localization and endocytic function of cubilin on visceral endoderm and kidney proximal tubules. *Development* **131**, 4787-4795. doi:10.1242/dev.01341

Tanner, S. M., Aminoff, M., Wright, F. A., Liyanarachchi, S., Kuronen, M., Saarinen, A., Massika, O., Mandel, H., Broch, H. and de la Chapelle, A. (2003). Amnionless, essential for mouse gastrulation, is mutated in recessive hereditary megaloblastic anemia. *Nat. Genet.* **33**, 426-429. doi:10.1038/ng1098

Tanner, S. M., Sturm, A. C., Baack, E. C., Liyanarachchi, S. and de la Chapelle, A. (2012). Inherited cobalamin malabsorption. Mutations in three genes reveal functional and ethnic patterns. *Orphanet J. Rare Dis.* **7**, 56. doi:10.1186/1750-1172-7-56

Teumer, A., Tin, A., Sorice, R., Gorski, M., Yeo, N. C., Chu, A. Y., Li, M., Li, Y., Mijatovic, V., Ko, Y.-A. et al. (2016). Genome-wide association studies identify genetic loci associated with albuminuria in diabetes. *Diabetes* **65**, 803-817. doi:10.2337/db15-1313

Tsurumi, H., Kurihara, H., Miura, K., Tanego, A., Ohta, Y., Igarashi, T., Oka, A., Horita, S., Hattori, M. and Harita, Y. (2016). Afadin is localized at cell-cell contact sites in mesangial cells and regulates migratory polarity. *Lab. Invest.* **96**, 49-59. doi:10.1038/labinvest.2015.133

Udagawa, T., Harita, Y., Miura, K., Mitsui, J., Ode, K. L., Morishita, S., Urae, S., Kanda, S., Kajiho, Y., Tsurumi, H. et al. (2018). Amnionless-mediated glycosylation is crucial for cell surface targeting of cubilin in renal and intestinal cells. *Sci. Rep.* **8**, 2351. doi:10.1038/s41598-018-20731-4

Wada, I., Rindress, D., Cameron, P. H., Ou, W. J., Doherty, J. J., II, Louvard, D., Bell, A. W., Dignard, D., Thomas, D. Y. and Bergeron, J. J. (1991). SSR alpha and associated calnexin are major calcium binding proteins of the endoplasmic reticulum membrane. *J. Biol. Chem.* **266**, 19599-19610.

Wang, M., Chen, J., He, K., Wang, Q., Li, Z., Shen, J., Wen, Z., Song, Z., Xu, Y. and Shi, Y. (2015). The NVL gene confers risk for both major depressive disorder and schizophrenia in the Han Chinese population. *Prog. Neuropsychopharmacol. Biol. Psychiatry* **62**, 7-13. doi:10.1016/j.pnpbp.2015.04.001

Yammani, R. R., Seetharam, S. and Seetharam, B. (2001). Identification and characterization of two distinct ligand binding regions of cubilin. *J. Biol. Chem.* **276**, 44777-44784. doi:10.1074/jbc.M106419200

Yoshikatsu, Y., Ishida, Y., Sudo, H., Yuasa, K., Tsuji, A. and Nagahama, M. (2015). NVL2, a nucleolar AAA-ATPase, is associated with the nuclear exosome and is involved in pre-rRNA processing. *Biochem. Biophys. Res. Commun.* **464**, 780-786. doi:10.1016/j.bbrc.2015.07.032

Zanetti, D., Rao, A., Gustafsson, S., Assimes, T. L., Montgomery, S. B. and Ingelsson, E. (2019). Identification of 22 novel loci associated with urinary biomarkers of albumin, sodium, and potassium excretion. *Kidney Int.* **95**, 1197-1208. doi:10.1016/j.kint.2018.12.017

Zhao, S. G., Evans, J. R., Kothari, V., Sun, G., Larm, A., Mondine, V., Schaeffer, E. M., Ross, A. E., Klein, E. A., Den, R. B. et al. (2016). The landscape of prognostic outlier genes in high-risk prostate cancer. *Clin. Cancer Res.* **22**, 1777-1786. doi:10.1158/1078-0432.CCR-15-1250

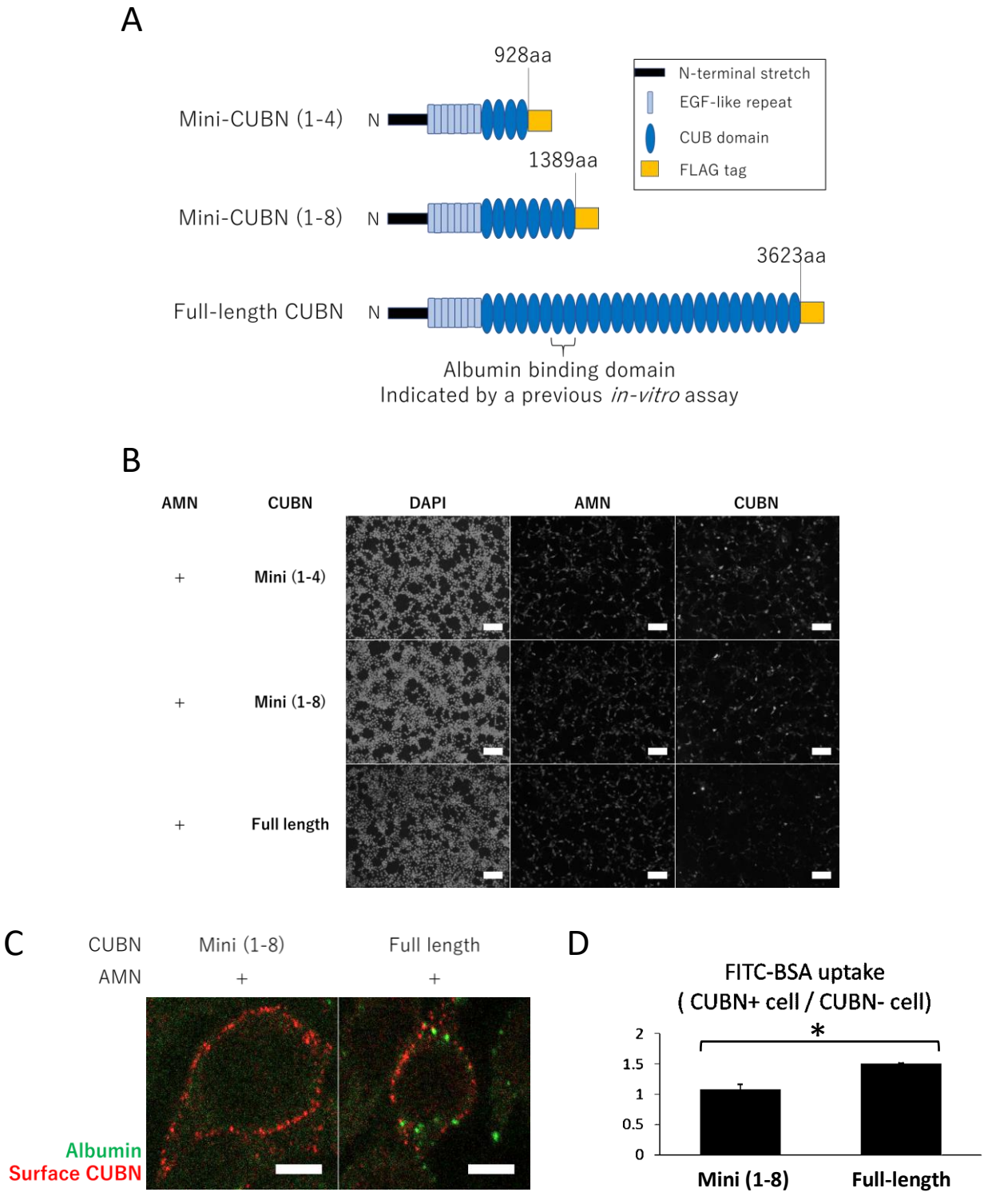

Figure S1. A CUBN segment stretching from the N-terminus to CUB 8 domain fails to facilitate cellular albumin uptake.

A Schematic representation of mini-CUBN (1–4), mini-CUBN (1–8), and full-length CUBN.

B Expression of FLAG-tagged mini-CUBN (1–4), mini-CUBN (1–8), and full-length CUBN co-expressed with myc-GFP-tagged AMN in HEK293T cells. Scale bar = 100 μm.

C FITC-albumin uptake by HEK293T cells expressing mini-CUBN (1–8) or full-length CUBN with AMN. Cells were immunostained for surface CUBN after FITC-albumin uptake. Scale bar = 5 μm.

D Flow cytometric quantification of FITC-albumin uptake by HEK293T cells expressing mini-CUBN (1–8) or full-length CUBN on their surface as in Figure 1E. Data are shown as mean ± s. e. m., n = 3. *$P < 0.05$, two-sided *t*-test.

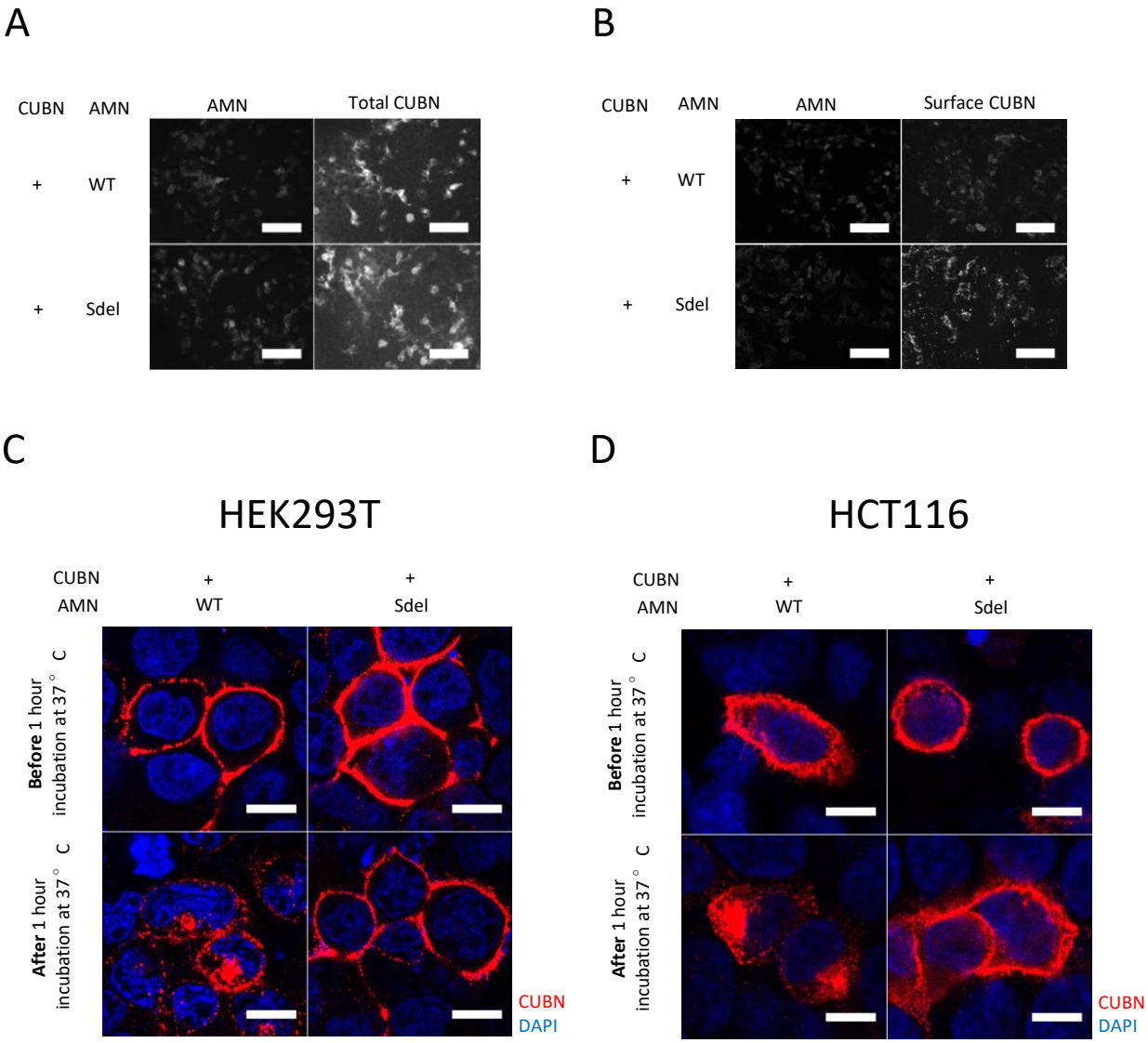

Figure S2. Signal motifs of AMN are critical for CUBN endocytosis in cells with or without endogenous megalin.
A, B Total expression (A) and membrane expression (B) of FLAG-tagged full-length CUBN in HEK293T cells co-expressing myc-GFP-tagged WT-AMN or Sdel-AMN. Scale bar = 100 μm.
C, D HEK293T (C) or HCT116 (D) cells were co-transfected with FLAG-tagged CUBN and myc-tagged WT-AMN or Sdel-AMN. FLAG-CUBN on the cell surface was detected before or after the endocytosis period (37° C, 1 h). Scale bar = 10 μm.

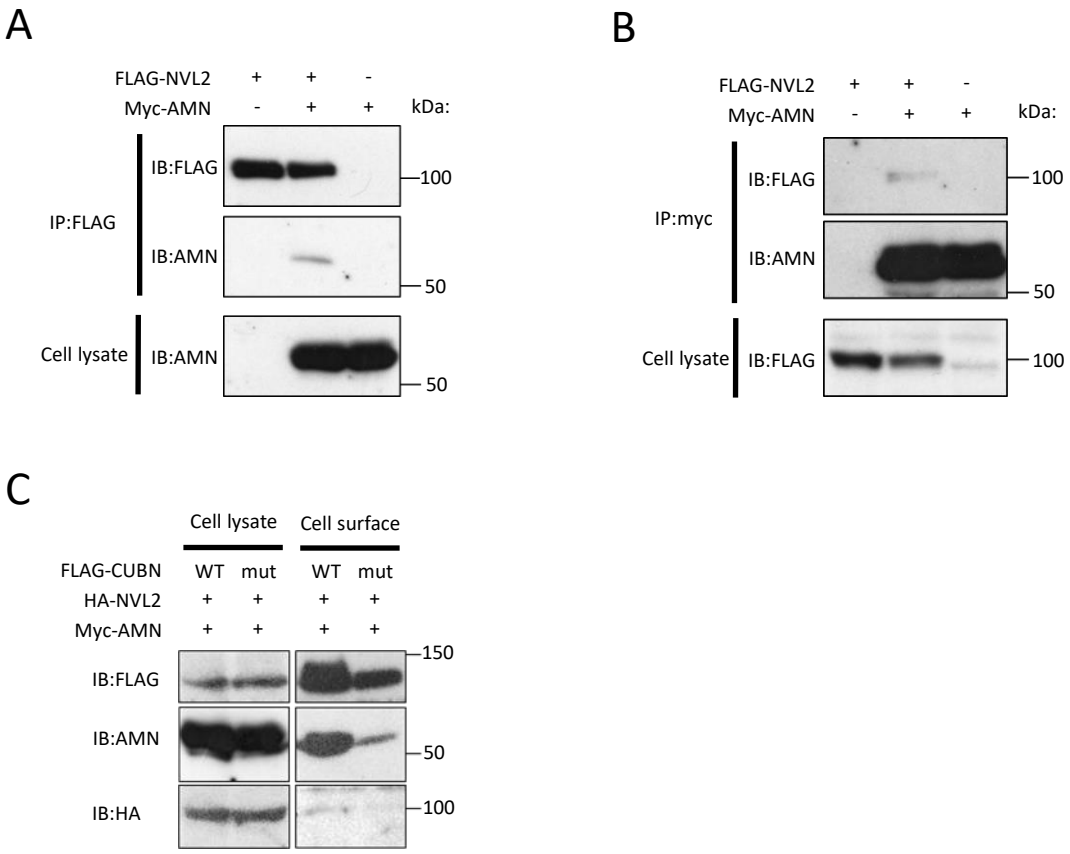

Figure S3. NVL2 interacts with AMN and CUBAM.

A, B Coimmunoprecipitation of myc-tagged AMN and FLAG-tagged NVL2 exogenously expressed in HEK293T cells.

C Immunoprecipitation of WT or mutant (G653R) CUBN expressed on the cell surface. FLAG-tagged CUBN on cell surface was labelled with anti-FLAG antibody in cultured medium and its bound proteins were analyzed by western blot.

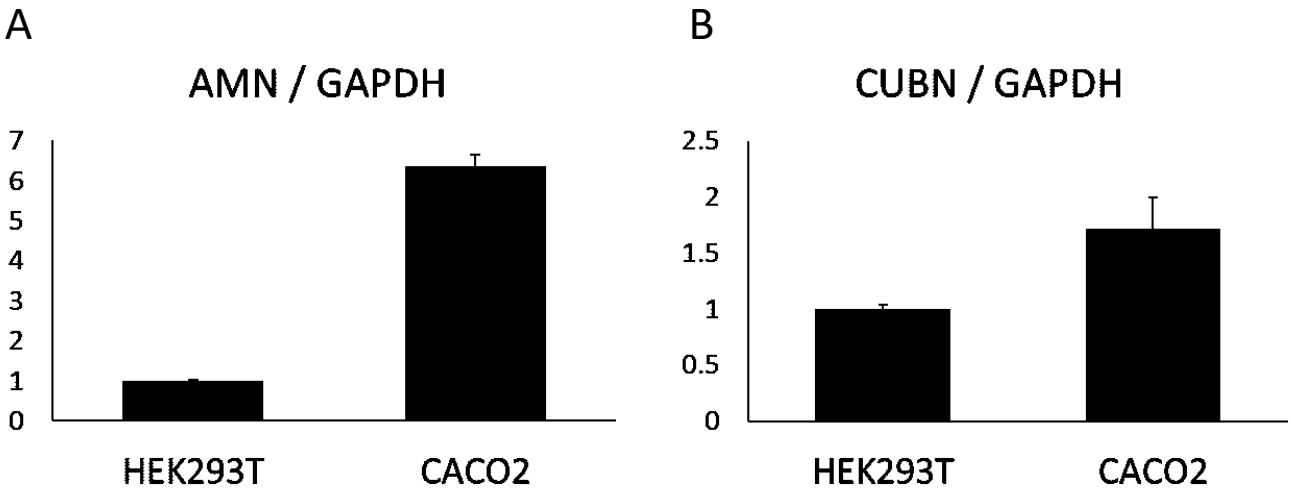

Figure S4. CACO2 cells, but not HEK293T cells, express endogenous AMN and CUBN mRNA.
A, B AMN (A) and CUBN (B) mRNA levels normalized to GAPDH mRNA in HEK293T and CACO2 cells were evaluated by qPCR.

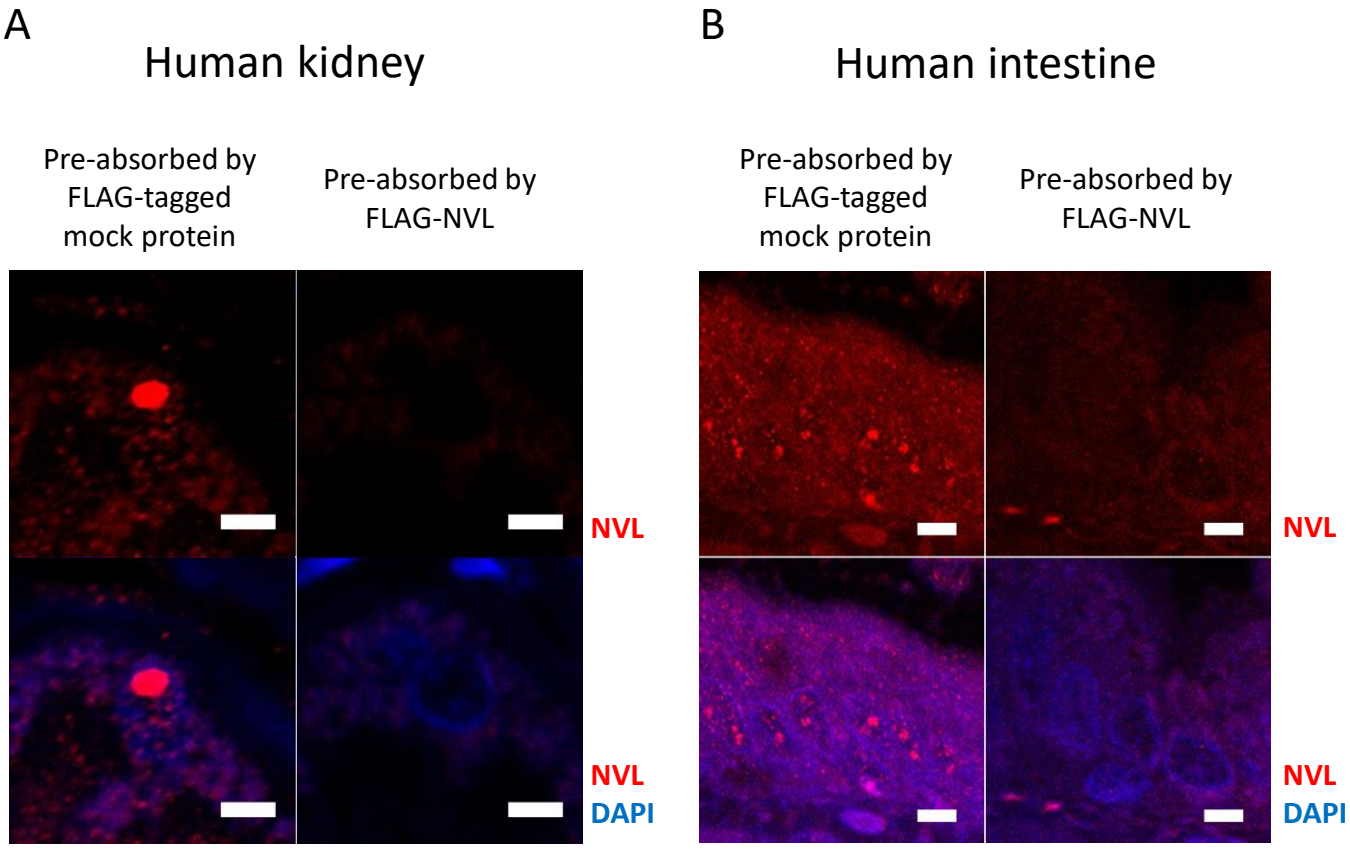

Figure S5. Immunofluorescence signals are specificity of signals for NVL in human kidney and intestine.
A, B Human kidney(A) and intestine(B) sections were immunostained with anti-NVL antibody pre-absorbed by anti-FLAG immunoprecipitates from lysates of HEK293T cells expressing FLAG-tagged negative control protein (FLAG-KLHL3) or FLAG-NVL2. Scale bar = 5 μm

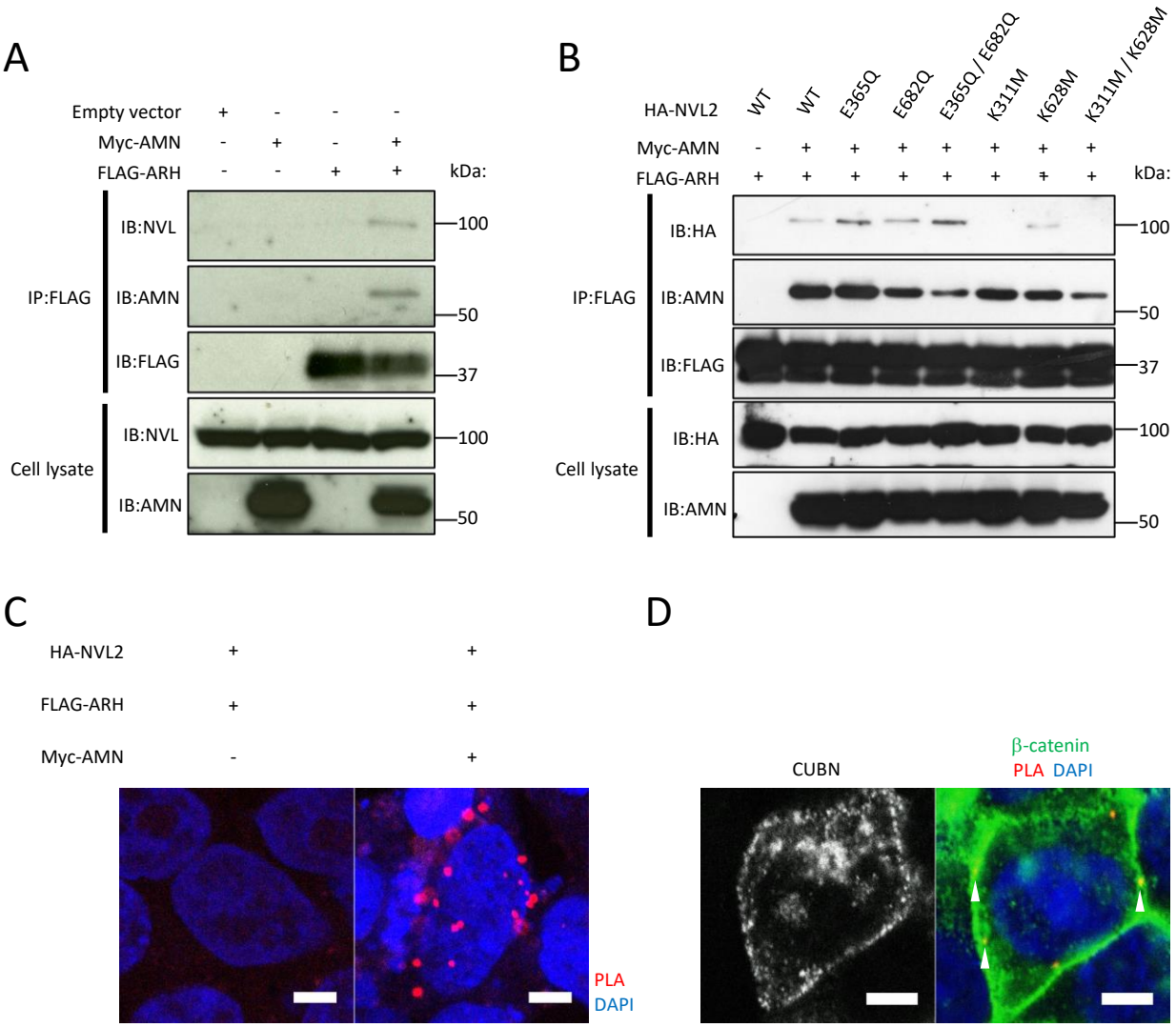

Figure S6. NVL2 forms a trimeric complex with ARH and AMN.

A Co-immunoprecipitation of endogenous NVL2 with exogenously expressed AMN and ARH in HEK293T. Cell lysates and anti-FLAG immunoprecipitates were analyzed using the indicated antibodies.

B Co-immunoprecipitation of HA-tagged WT or mutant NVL2 with AMN and ARH exogenously expressed in HEK 293T cells.

C In situ PLA of HA-tagged NVL2 and FLAG-tagged ARH in HEK293T cells with or without AMN coexpression. Scale bar = 5 μm.

D In situ situ PLA of HA-tagged NVL2 and FLAG-tagged ARH in HEK293T cells coexpressing myc-tagged AMN and GFP-tagged CUBN. Cells were immunostained for β-catenin after the PLAs. Scale bar = 5 μm.

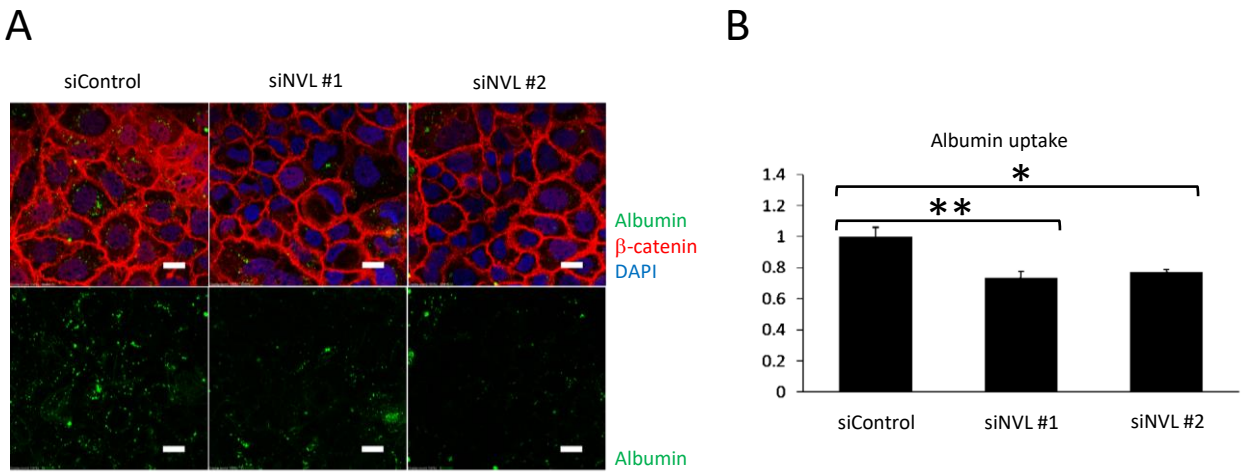

Figure S7. NVL depletion reduces albumin uptake in CACO2 cells.
A FITC-albumin uptake by CACO2 cells transfected with the indicated siRNAs. Cells were immunostained for b-catenin after FITC-albumin uptake. Scale bar = 20 μm.
B Quantification of FITC-albumin uptake by CACO2 cells transfected with the indicated siRNAs. Median FITC signal intensity of each cell group was measured by flow cytometry. Data are shown as mean ± s. e. m., n = 6. **P*<0.05, ***P*<0.01, two-sided *t*-test.

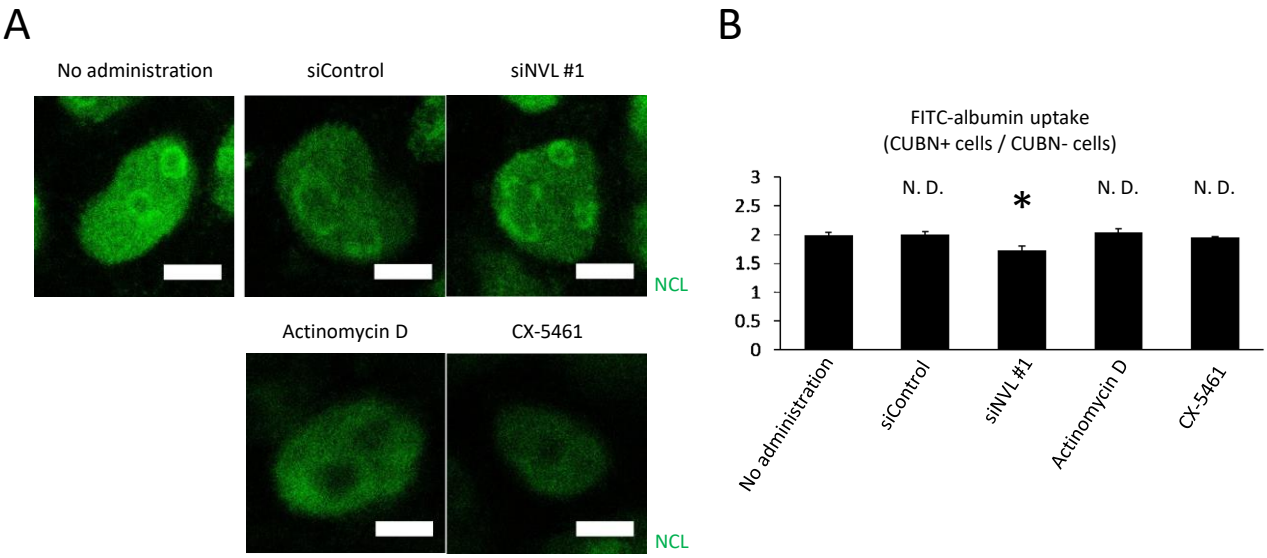

Figure S8. NVL2 promotes albumin endocytosis independently of nucleolar stress.
A Localization of nucleolin (NCL) in HEK293T cells transfected with siNVL, or incubated with media containing actinomycin D or CX-5461. Scale bar = 5 μm.
B Flow cytometric quantification of FITC-albumin uptake in HEK293T cells transfected with siNVL, or incubated with media containing actinomycin D or CX-5461 as in Figure 1E. Data are shown as mean ± s. e. m., n=3. N. D. = no difference, *P < 0.05, two-sided t-test.